Fusion Engineering and Design 173 (2021) 112933

Contents lists available at ScienceDirect

Fusion Engineering and Design

journal homepage: www.elsevier.com/locate/fusengdes

Integrated design of breeding blanket and ancillary systems related to the use of helium or water as a coolant and impact on the overall plant design

G.A. Spagnuolo [a,*], R. Arredondo [b], L.V. Boccaccini [c], P. Chiovaro [d], S. Ciattaglia [a], F. Cismondi [e], M. Coleman [f], I. Cristescu [c], S. D'Amico [c], C. Day [c], A. Del Nevo [g], P.A. Di Maio [d], M. D'Onorio [h], G. Federici [a], F. Franza [c], A. Froio [i], C. Gliss [a], F.A. Hernández [c], A. Li Puma [j], C. Moreno [k], I. Moscato [a], P. Pereslavtsev [c], M.T. Porfiri [g], D. Rapisarda [k], M. Rieth [c], A. Santucci [g], J. C. Schwenzer [c], R. Stieglitz [c], S. Tosti [g], F.R. Urgorri [k], M. Utili [g], E. Vallone [d]

[a] EUROfusion Consortium, Programme Management Unit, Garching, Germany
[b] Max-Planck-Institut für Plasmaphysik, Garching, Germany
[c] Karlsruhe Institute of Technology, Eggenstein-Leopoldshafen, Germany
[d] Dipartimento di Ingegneria, Università di Palermo, Palermo, Italy
[e] Fusion for Energy (F4E), Rokkasho, Japan
[f] United Kingdom Atomic Energy Authority, United Kingdom
[g] Fusion and Technology for Nuclear Safety and Security Department, ENEA, Italy
[h] DIAEE, Sapienza University of Rome, Roma, Italy
[i] NEMO Group, Dipartimento Energia, Politecnico di Torino, Torino, Italy
[j] Commissariat à l'énergie atomique et aux énergies alternatives (CEA), Saclay, France
[k] CIEMAT, Fusion Technology Division, Madrid, Spain

ARTICLE INFO

Keywords:
Breeding blanket
Integration issues
Water activation
Tritium management
VVPSS

ABSTRACT

Currently, for the EU DEMO, two Breeding Blankets (BBs) have been selected as potential candidates for the integration in the reactor. They are the Water Cooled Lithium Lead and the Helium Cooled Pebble Bed BB concepts. The two BB variants together with the associated ancillary systems drive the design of the overall plant. Therefore, a holistic investigation of integration issues derived by the BB and the installation of its ancillary systems has been performed. The issues related to the water activation due to the ^{16}N and ^{17}N isotopes and the impact on the primary heat transfer systems have been investigated providing guidelines and dedicated solution for the integration of safety devices as isolation valves. The tritium retention and the permeation rates through the blanket and its ancillary systems have been also assessed taking into account different operating points both for the BB and ancillaries and comparing, when possible, the releases with the operating and safety limits. Moreover, the issues related to the tritium start-up inventory as well as the uncertainties on the Tritium Breeding Ratio (TBR) due to the integration of the auxiliary systems within the Vacuum Vessel have been also studied. Finally, the impact of the BB concepts on the safety systems like the Vacuum Vessel Pressure Suppression System is described with a particular focus on the different measures that should be implemented according to the considered concept. All these aspects are then taken into account to drive future developments during the Concept Design Phase.

1. Introduction

Within the framework of the EUROfusion consortium activities, the development of a fusion EU DEMO reactor (that will be simply called DEMO in the rest of the paper), which should achieve long operation time, demonstrate tritium self-sufficiency and demonstrate a net electricity output, is pursued [1,2]. DEMO represents a step forward with respect to the ITER reactor and it will pose the basis for the construction of a Fusion Power Plant (FPP) as defined in [3,4]. The EUROfusion consortium has concentrated its efforts on the holistic investigation of

* Corresponding author.
E-mail address: alessandro.spagnuolo@euro-fusion.org (G.A. Spagnuolo).

https://doi.org/10.1016/j.fusengdes.2021.112933
Received 4 August 2021; Received in revised form 27 October 2021; Accepted 8 November 2021
Available online 17 November 2021

integration issues that, as demonstrated in ITER, represent one of the most complicated challenges for a complex machine like DEMO. In this regard, eight Key Design Integration Issues (KDIIs) have been identified in [5].

In this paper, the work performed in KDII2, namely on the integration issues related to the Breeding Blanket (BB) and its ancillary systems, is described. It deals with the integrated design of blanket ancillary systems related to the use of helium or water as coolants for the blanket and its impact on the overall plant design. Particular focus is given to the issues connected to the BB variants in terms of (i) impact on the overall plant design (Section 2), (ii) radiation protection measures due to the BB integration (Section 3), (iii) management of tritium (Section 4) and (iv) impact on the safety (Section 5). Indeed, assuming that all the BB variants show similar performances and satisfy the System Requirement, it is worth to analyse the issue connected to the integration. Therefore, the scope of this work is to identify the potential integration issues and the possible solutions that should be further investigated. However, the topics herewith presented are not meant to be exhaustive but, on the contrary, they represent the best knowledge at the moment developed within EUROfusion, during the Pre-Concept Design Phase, and that will be used for the next Concept Design Phase. Furthermore, although these topics are not addressing all the challenges associated with the BB selection, they have been identified to be the most important ones due to their impact on the DEMO plant design.

2. Integration issues and impact on the overall plant design

In this study, the two BB variants (i.e. Water Cooled Lithium Lead, WCLL, and Helium Cooled Pebble Bed, HCPB) share several features dictated by the use of common DEMO architecture (see [1]) during the Pre-Concept Design Phase. Indeed, both blankets systems are subdivided into 16 sectors (according to the number of Toroidal Field coils), each of them is further subdivided into 5 segments (two inboards and three outboards). EUROFER97 (reduced activation ferritic-martensitic steel) is used as a structural material for both concepts. Each segment is composed of subcomponents like the First Wall (FW) facing directly the plasma, a Back Supporting Structure (BSS) with the function to support, and a Breeder Zone (BZ) housing breeder and multiplier materials. Furthermore, both concepts have to fulfil the same functions in terms of (i) tritium production (to keep the self-sufficiency of the reactor), (ii) heat removal (to transfer the power to the Power Conversion System (PCS) at thermal-hydraulic conditions suitable for electricity production) and (iii) radiation shielding of the Vacuum Vessel (VV) and magnet system [6,7].

On the other side, according to each BB concepts, some differences may occur. These differences are mainly related to the type of coolant (e.g. water or He), thermal-hydraulic conditions, kind of neutron multiplier and breeder materials and Tritium-carrier (T-carrier). These features affect the development of the ancillary systems interfacing the BB, such as the Primary Heat Transfer System (PHTS), Coolant Purification System (CPS), Tritium Extraction and Removal System (TER), etc. requiring different technologies. Thereby, the selection of the BB concepts impacts the overall DEMO plant architecture and, consequently, the design solutions to be implemented.

In the following paragraph, more information about the two DEMO variants deriving from the selection of the BB is reported.

2.1. The WCLL breeding blanket and its ancillary systems

The WCLL BB [8,9] relies on the use of eutectic alloy $Pb_{83}Li_{17}$ enriched at 90% in ^{6}Li as a tritium breeder, neutron multiplier and tritium carrier, Eurofer as a structural material. The blanket is cooled by water at 15.5 MPa, with an inlet temperature of 295 °C and outlet temperature of 328 °C, flowing into two independent systems, the FW and the BZ coolant systems [10]. The FW coolant flows in square channels in a counter-current direction. The water coolant of the BZ system flows in radial-toroidal Double Walled Tubes (DWTs). The internal structure consists of radial-poloidal and radial-toroidal stiffening plates: the same modular structure (breeding unit) is repeated in the poloidal direction. The PbLi flows in the breeding unit in the radial-poloidal direction.

The WCLL BB PHTS has the function to remove thermal power from the BB and to deliver it to the secondary circuit through the main heat transfer equipment. Depending on the Balance of Plant (BoP) solution employed [11], the secondary circuit can be either an Intermediate Heat Transfer System (IHTS) equipped with an Energy Storage System ESS, which thermally decouples the PHTS to the PCS, or directly the PCS [12,13]. As consequence, the main heat transfer equipment of the PHTS can be either steam generators (SG) or Intermediate Heat eXchangers (IHX). The WCLL BB PHTS is divided into two independent primary systems: the BZ PHTS and the FW PHTS. Each primary circuit has two cooling loops, each feeding eight tokamak sectors via annular feeding rings. The main components are located on two opposite sides of the tokamak building. The coolant pumps are located nearby the heat exchanger exit. A short pipe connects the pumps to the heat exchanger; downstream, the coolant pump is connected to the cold leg [14]. All investigated BoP solutions rely on the direct coupling of the BZ PHTS to the PCS via SGs. On the contrary, one variant conceives that FW PHTS transfers its thermal power to the IHTS, which in turn delivers the heat to the PCS (see Fig. 2).

The CPS unit treats a by-pass of the primary coolant to maintain the tritium and the impurity content below certain values. Due to the difficulties in realizing and operating detritiation systems with large flow rates for the decontamination of tritiated water with low (or very low) activity level, the amount of coolant routed inside the CPS should stay below the technological limit currently identified in the largest existing water detritiation system (i.e. the Darlington tritium removal facility designed to process a tritiated water flow of 360 kg/h). The solution proposed for the tritium removal from water coolant is the Combined Electrolysis and Catalytic Exchange (CECE) process which foresees the use of an electrolyser and a liquid phase catalytic exchange column. However, due to the significant permeation rate into water coolant, the sole use of a water detritiation system (even one having the largest existing size) does not allow the necessary tritium removal rate. Therefore, the tritium control in water coolant has to be achieved by a proper combination of effective anti-permeation barriers and CPS by-pass [15,16].

The WCLL TER system recirculates outside the VV the PbLi using dedicated loops for transporting the tritium to the extraction units; there, the tritium is routed to the Tokamak Exhaust Processing of the Fuel Cycle. Its main functions are:

- To circulate the liquid PbLi through the BB and to extract the tritium produced inside therewith.
- To provide adequate heating to maintain PbLi liquid in all system locations, including BB.
- To control PbLi chemistry and remove accumulated activated impurities.
- To ensure gravitational draining of the BB and the PbLi loops.
- To accommodate possible overpressures of the liquid metal.

The WCLL TER system is subdivided into 4 loops for the Outboard Blanket (OB) segments and 2 loops for the Inboard Blanket (IB) segments, respectively (Fig. 1). The total amount of PbLi for each loop is 50 and 232 m^3 for the IB and OB, respectively. During non-operation phases, the PbLi is recovered in dedicated tanks placed in the lower part of the circuit to allow draining by gravity. The TER operates at a temperature of ~328 °C with a total mass flow rate of 874 kg/s for the OB loops and 163 kg/s for the IB loops, respectively. The maximum PbLi speed is 0.5 m/s while the maximum operating pressure is equal to 4.6 MPa.

It is easy to understand that several interactions in terms of heat and

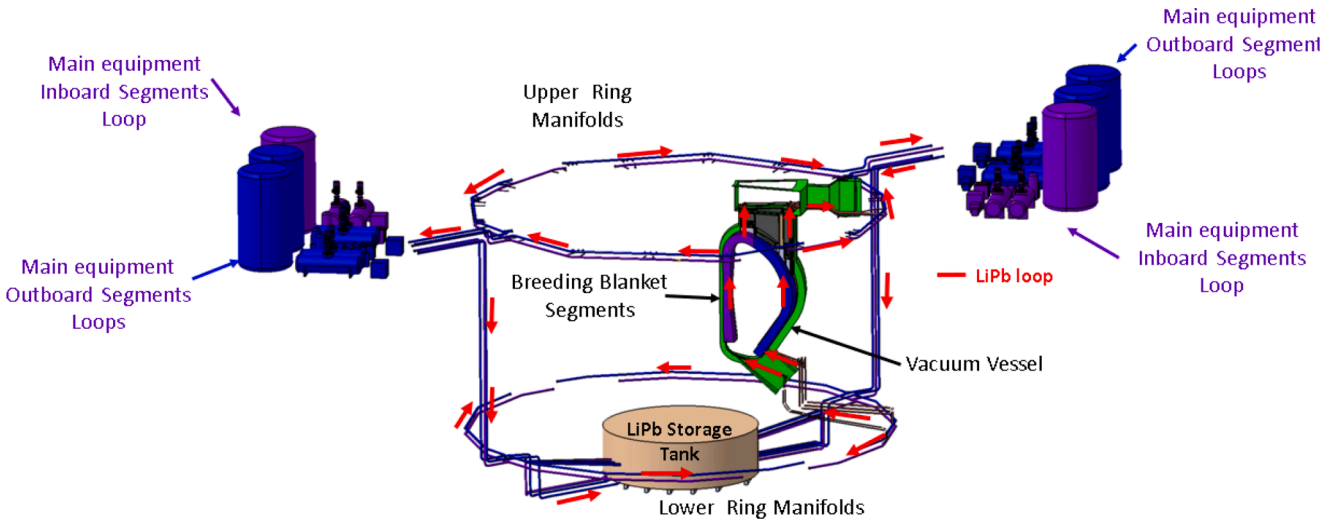

Fig. 1. 3-D drawing of the PbLi loops integrated within DEMO building.

mass transfer occur between the BB and the ancillary systems both during normal and accidental conditions (i.e. heat transfer and tritium mass transfer occur in parallel, therefore, since both processes are controlled and positively influenced by the same parameters such as temperature, pressure and surface area, it results that the optimum blanket design under the heat transfer point of view could not control very well the *T* permeation). An example of the heat and tritium transfer among the different systems is reported in Fig. 2.

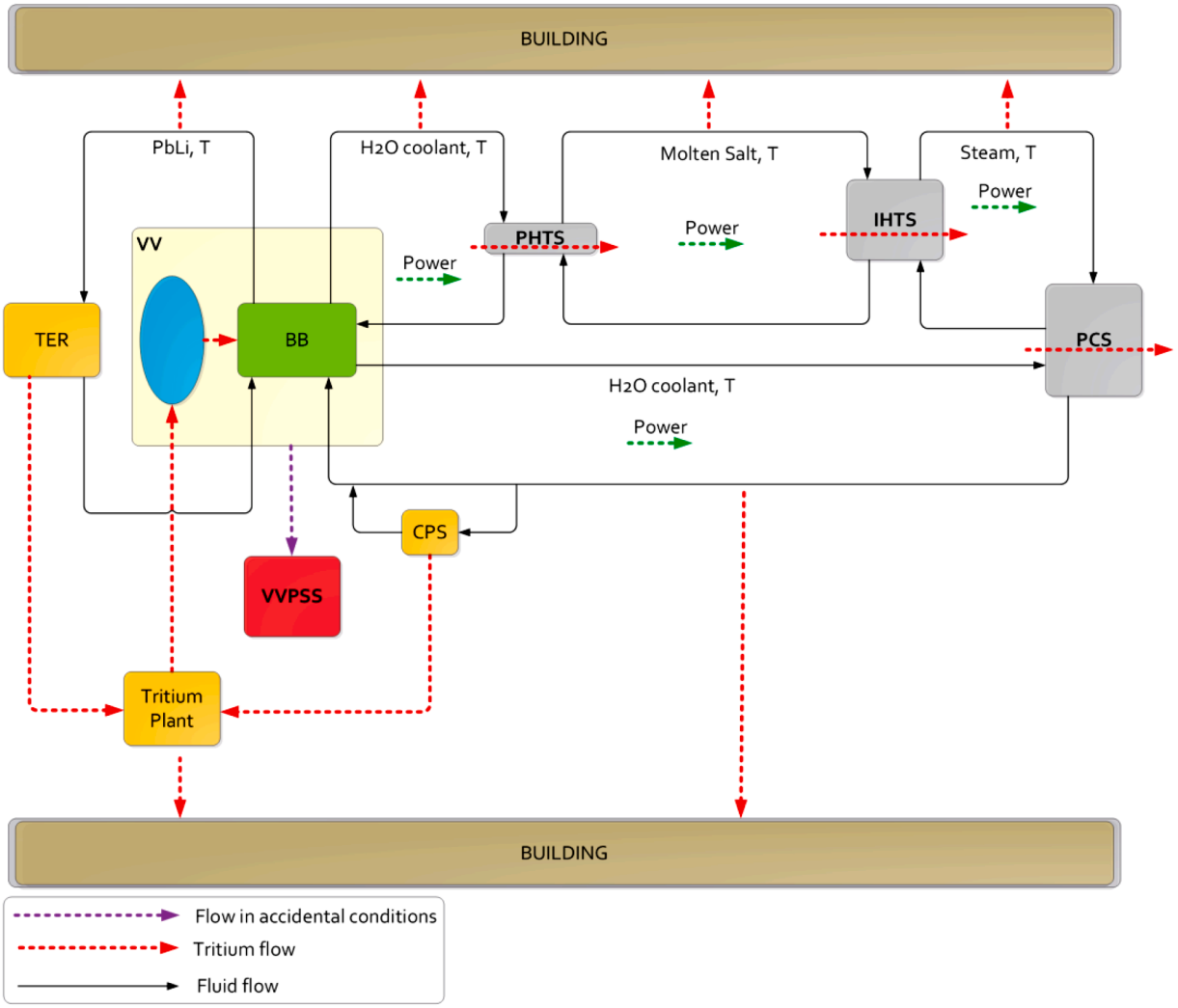

Fig. 2. Schematic drawing of the tritium and heat removal paths of the Water-cooled DEMO architecture.

2.2. The HCPB breeding blanket and its ancillary systems

The HCPB BB (Fig. 3) [8] relies on the use of Ceramic Breeder (CB) in the form of Li_4SiO_4+35 mol%Li_2TiO_3 pebbles as tritium breeder material enriched at 60% in ^{6}Li. Hexagonal beryllide ($Be_{12}Ti$) prismatic blocks are used as neutron multiplier. Helium is used both as coolant (@80 bar, inlet temperature of 300 °C and outlet temperature of 520 °C) and T-carrier (@2 bar doped with an additional hydrogen content of 300 Pa, i.e. ~0.1% wt. H_2) [10]. The current design [17] is based on a radial arrangement of so-called fuel-breeder pins containing CB material and attached to the FW. Each beryllide block is supported by its corresponding fuel pin through a spacer, thus filling in this way the space between fuel pins. The helium coolant first flows from the FW inlet manifold to the FW cooling channels (counter-current flow). The coolant is then collected and it is mixed in the BZ inlet manifold. The coolant is then distributed into the fuel pins in the BZ. The coolant is collected from the pins in the outlet plenum and redirected to the BZ outlet (i.e. BSS outlet piping) [18,19].

Concerning the HCPB PHTS, four concepts were preliminarily conceived as suitable to accomplish DEMO HCPB BOP needs. One of them foresees an indirect coupling of the BB PHTS to the PCS, interposing in between them an IHTS equipped with an ESS to cope with the lack of fusion power during dwell time [11]. The main function of the HCPB BB PHTS is to extract thermal power from the BB components and transfer it to an IHTS through the IHXs [12,13]. The whole HCPB BB PHTS envelope encloses the primary coolant and has the function of providing primary confinement for tritium and activated particles (if any) carried by helium and maintaining leak-tight integrity during all system states. The HCPB BB PHTS concept is based on the use of pressurized helium as a coolant medium at about 8 MPa and inlet/outlet temperatures of 300/520 °C. Each of the 8 cooling loops feeds 2 BB sectors made of 10 blanket segments, 4 IBs and 6 OBs, respectively. Each cooling loop consists of: In-VV BB cooling circuits belonging to two VV sectors, an IHX, two circulators, and the connecting piping between these components. The eight IHXs are located on two opposite sides in the tokamak cooling rooms on the upper level of the tokamak building. On one location all IHXs are located in a row and equally distributed. The helium circulators are located near the bottom head of the IHXs; two short pipes, upstream and downstream of each circulator, connect the component to the IHX and the cold leg, respectively [11].

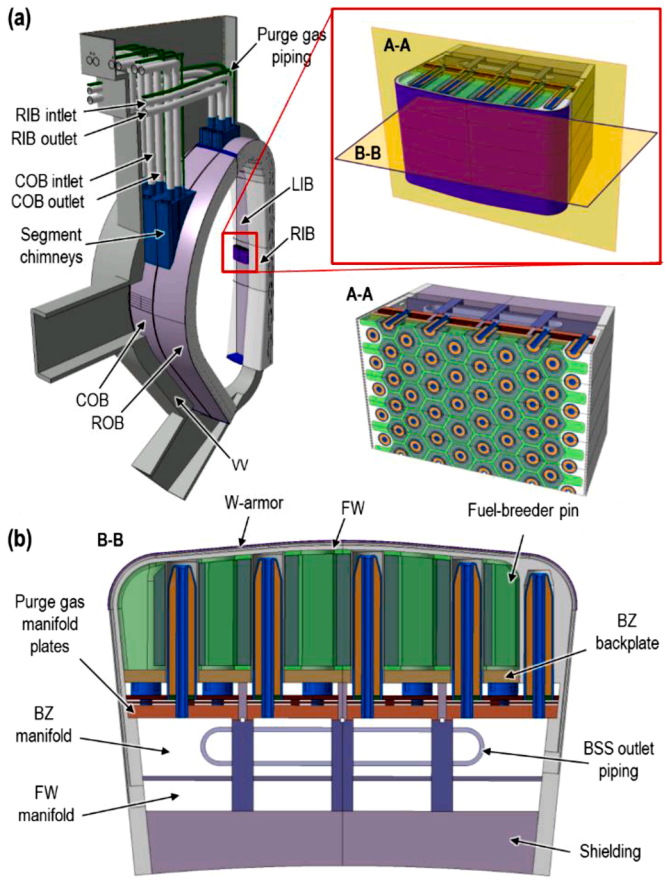

Fig. 3. Section views of a lateral IB segment of the HCPB concept [17].

The CPS is composed of two sub-systems: one for the removal of the hydrogen isotopes and one for the removal of other impurities. The latter is composed of a combination of filters and non-regenerable getters for which the design can be improved only when additional data on the impurities amount and composition will be available. The unit for the hydrogen isotopes removal is based on the scale-up of the conventional process used in fission and also in ITER CPS which comprises the following steps: (i) Q_2 (Q being one of the hydrogen isotopes) into Q_2O oxidation via copper oxide beds, (ii) Q_2O removal from helium using molecular sieves and, (iii) treatment of the desorbed Q_2O in reducing beds or through the water detritiation system. The main advantage of this process is that it uses relatively mature and consolidated technologies. However, some drawbacks arise due to the use of several technologies requiring frequent regeneration with the contemporary presence of O_2 and Q_2 species and the necessity to double the number of components to allow the regeneration. To overcome this issue, an alternative process has been also considered which relies on the use of novel non-evaporable getter (NEG) material (named ZAO alloy) which allows the direct adsorption of the Q_2 from the helium stream. Due to the novelty of this material, dedicated experiments are required to assess its efficacy under DEMO relevant conditions [15,16].

The HCPB TER system relies on helium purge gas with an addition of 0.1% wt. H_2 as a doping agent to promote isotopic exchange between T in functional materials and H_2. The inlet temperature at the BB segments is ≈300 °C. The purge gas flow rate has been conservatively set at 10,000 Nm^3/hr, which has been used as well for the pre-concept design of the HCPB TER. The resulting plant purge gas mass flow rate is 0.5 kg/s, resulting in a reasonable TER system size ready for its industrialization. On the other side, this purge gas flow rate is considered to be low enough not to extract any significant amount of power from the BB. The TER HCPB consists of the following main components:

- Reactive Molecular Sieve Beds (RMSB). Presently two RMSBs are included in the TER HCPB: one RMSB is in the adsorption phase and the second in the regeneration phase. The scope of the RMSB is to adsorb the tritiated water vapours from the purge gas and to realize the isotopic exchange because of tritium recovery during the regeneration process. The isotopic exchange is realized between the tritiated vapours adsorbed on the RMSB and an H_2/D_2 swamping stream provided from the Tritium Plant (TP). The H_2/D_2 stream is circulated in a closed loop between the TER and TP having the duty to transport tritium from the TER RMSB to the TP.
- Cryogenic Molecular Sieve Beds (CMSB). Two CMSB are required: one CMSB is in the adsorption phase and the second CMSB is in the regeneration phase. The regeneration of the CMSB is realized by increasing in a controlled manner the temperature in the sieve beds. The CMSBs are directly connected with a buffer vessel that shall provide two functions: mitigate the possible picks on the released gas from the CMSB during the warming–up of the molecular sieve beds and in addition to allow discharging of the CMSB inventory in the cases of uncontrolled warming up of the molecular sieve beds.
- The helium compressor that provides the required flow rate at 0.2 MPa.
- Heat exchangers that provide the operation temperatures of various components by energy recovery.
- Auxiliaries components/subsystems that provide controlled regeneration of the RMSB and CMSB and overpressure discharge.

- Connecting pipes and the instrumentation.

The tentative arrangement of the HCPB TER in the Tritium Building, the size and the internal configuration of the RMSB and the CMSB are shown in Fig. 4.

A schematic representation of the interaction between the Helium-cooled DEMO architecture with a particular focus on the power transport and tritium flows is reported in Fig. 5.

3. Radiation protection measures due to the BB

According to the BB concept that is used to equip DEMO, different challenges in terms of radiation protection measures have to be faced. They can be related to the PHTS that can become a distributed photon and neutron source due to the activation of water, or to the shielding performances of the BB concerning the VV and the magnet system. These issues have been investigated within the KDII2 using a holistic approach that takes into account the interconnections between the BB response and the different systems involved. More details are reported in the following paragraphs.

3.1. Water activation

The first step of the work has been to evaluate the spatial distribution of nitrogen isotope concentrations (^{16}N and ^{17}N) in the WCLL BB cooling circuits. To this purpose, a coupled neutronic/fluid-dynamic problem is solved following a theoretical approach and adopting an integrated computational tool mainly relying on the use of MCNP6 and ANSYS CFX codes. The adopted operative procedure foresees the assessment of the production rate distributions of nitrogen isotopes within FW and BZ cooling channels and tubes performing heterogeneous neutronic analyses. A fully 3-D fluid-dynamic approach is, then, used to compute the nitrogen isotope concentrations within the In-Vessel complex flow domain, while a 1-D lumped parameters approach is adopted to calculate their distribution along the Ex-Vessel BB PHTS [20]. Obtained results provided the necessary data to perform dedicated neutronic and photonic transport analyses and, hence, to assess the absorbed dose around some key components of the WCLL BB cooling circuit focusing the attention on the isolation valves. Therefore, the second step of the work has been focused on the assessment of the spatial distribution of the absorbed dose in the DEMO Upper Pipe Chase (UPC), focusing on the space neighbouring a typical isolation valve of the PHTS. To this end, a computational approach has been followed adopting the MCNP5 Monte Carlo code. In particular, a heterogeneous neutronic model of a portion of the UPC has been set up, including the valve and the main FW and BZ PHTS piping, and the spatial distribution of nitrogen isotopes concentrations, previously assessed, have been used to model the photonic and neutronic sources [21]. Finally, since the obtained results show that high dose values are reached in the aforementioned locations, simple design solutions to mitigate the absorbed dose have been studied. Furthermore, also their shielding performances have been assessed to provide adequate design solutions [22]. Regarding the study related to the 2020 PHTS design (Fig. 6), results show that the dose rate values in the valve are very close or greater than its failure threshold value (2 MGy, considering a life of 6,7 full power years (fpy) for the blanket) and in any case, such values are high in all the region of the UPC taken into account (Fig. 7). However, one can infer that the intensity of the dose field is such that there is a wide enough margin to find adequate solutions for the use of gate valves.

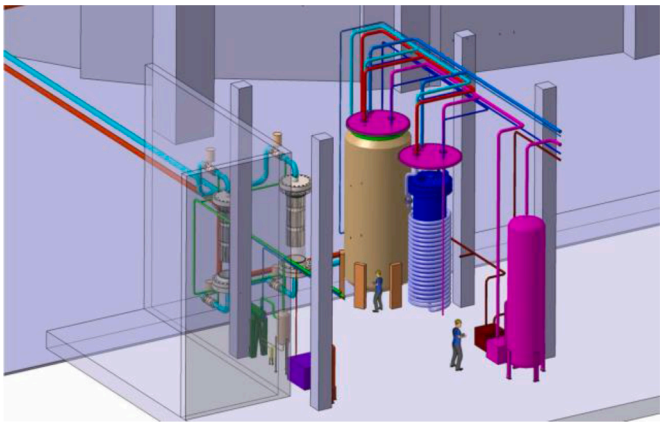

Fig. 4. Main HCPB TER in the tritium plant building.

The complexity of the current PHTS design and the dose rate levels calculated in UPC suggest that solutions such as bulkheads and boxes, previously considered for the UPC 2018 design, are not feasible due to the encumbrance they entail together with the lack of space in the UPC crowded with numerous pipes. Probably, the best way to ensure the availability of the valve throughout the blanket life is to adopt a strategy articulated in different actions with the least possible impact in the whole design, to minimize the integration issues. In compliance with thermal-mechanic and hydraulic limits, the velocity of water could be increased in the blanket (where it is irradiated) and slowed down, as much as possible, in the section of the PHTS circuits between the blanket and the UPC (however, this solution implies an increase of the volume and, therefore, of the inertia in the cooling system). Of course, parallel/cooperative actions could be both a proper relocation of the valve and the development of more rad-resistant material [23].

3.2. VV shielding

It is known that the HCPB BB is less performing than the WCLL BB in terms of shielding performances. Indeed, the shielding performance of this BB is about the limit set for the TF coils (< 50 W/m^3) at the equatorial IB side (Fig. 8) [24]. The neutron flux at $E_n > 0.1$ MeV in the superconducting magnet, in this case, is $\approx$7E + 08 n/cm^2 s, which corresponds to a neutron fluence of $\approx$1E + 21 n/m^2 during the full lifetime of the magnet. This is below the design limit of 1E + 22 n/m^2 after 6 fpy. The displacement per atom (dpa) damage accumulation in the VV (1.2 dpa/6 fpy) meets the requirement of $<$ 2.75 dpa). The maximum helium accumulation behind the VV does not exceed the design limit of 1 ppm for locations that may need pipe welding operations [25].

However, on the other side, the activation of the VV is a cause of increased concern in terms of waste disposal. The target value for the VV activity has not been yet assigned in the EUROfusion project, but the ALARA principle is assumed.

To reduce the potential hazard from the VV activation several shielding materials and arrangements (inside vs. outside of the BB, Fig. 9) have been investigated. Metal hydrides of Y, Zr and Ti and carbides of W and B are the most efficient shielding materials, contributing to the mitigation of the nuclear damage accumulation in the VV. The option of an 18 cm thick plate of TiH_2, $ZrH_{1.6}$, $YH_{1.75}$ or B_4C arranged behind the BSS results in a 10-fold decrease of radiation damage in the VV [25].

However, it is worth noting that the integration within the HCPB BB of these shielding materials poses additional integration challenges that need to be solved taking into account also the issues related to the temperature control of these materials, tritium accumulation as well as mechanical behavior and manufacturing procedures.

4. Management of tritium

The T managements in a complex machine like DEMO depends on the performances of the different systems that are involved (e.g. T extraction efficiency in TER system, by-pass mass flow rates in CPS, etc.) as well as on the design solutions that are implemented (off-line/on-line CPS, permeation barriers, etc.). All these parameters contribute to the

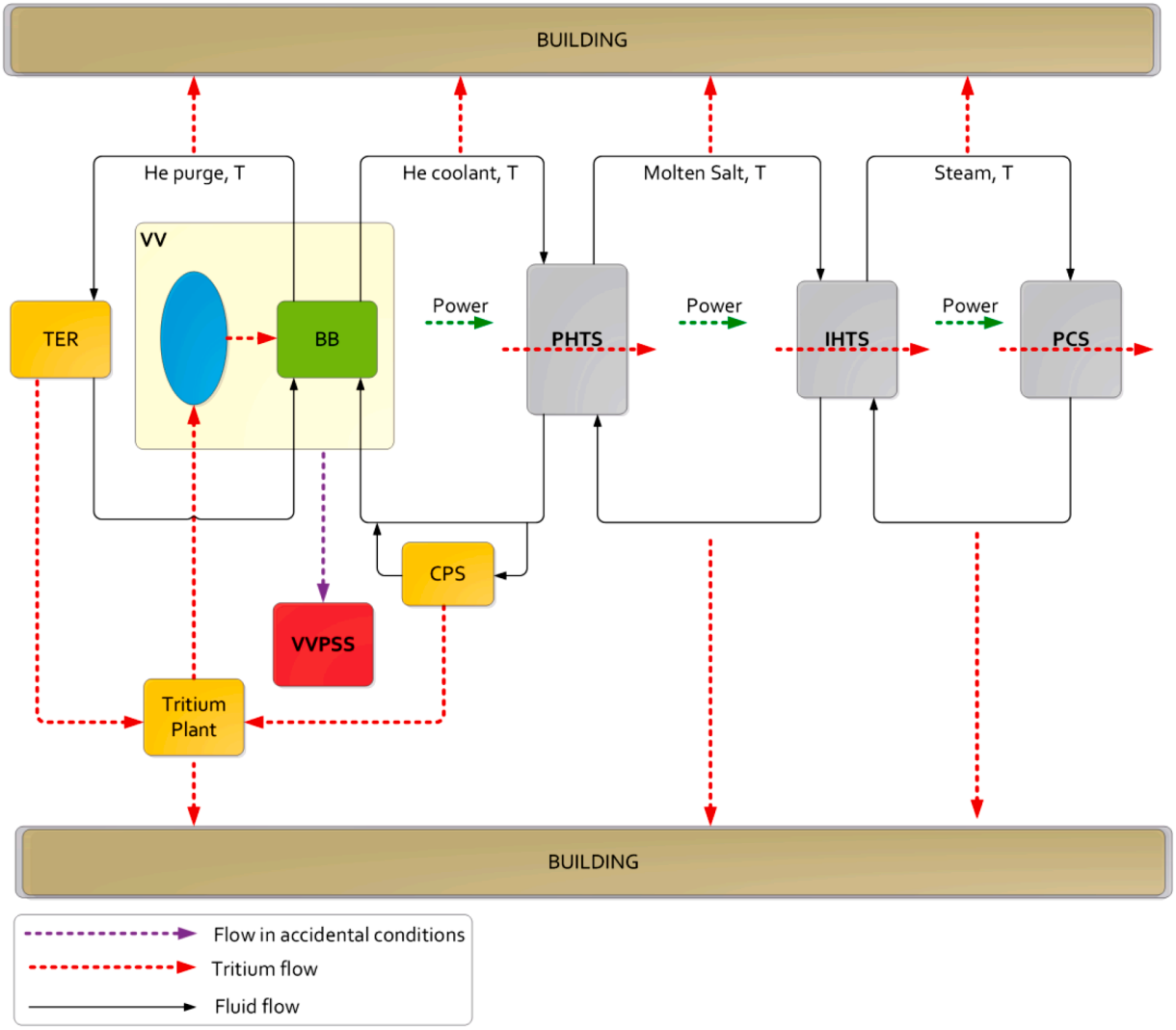

Fig. 5. Schematic drawing of the tritium and heat removal paths of the Helium-cooled DEMO architecture.

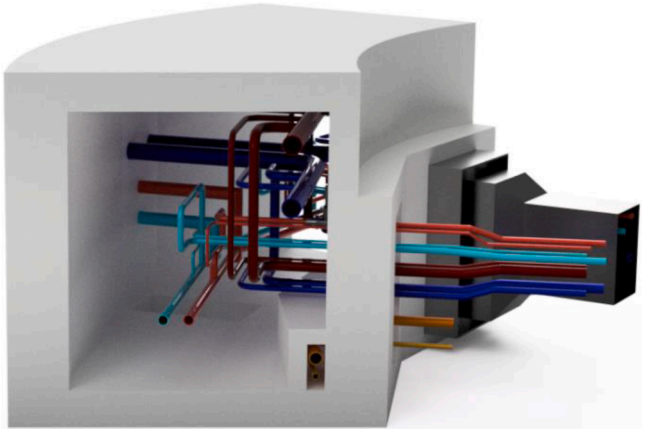

Fig. 6. DEMO PHTS CAD model of the UPC.

determination of the tritium inventories and releases being of potential safety concern.

In the following paragraphs, an overview of the main impacting system parameters is reported.

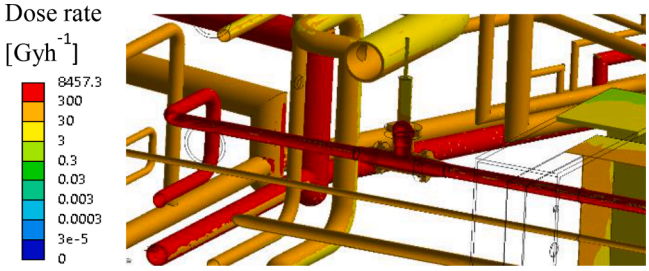

Fig. 7. Absorbed γ dose spatial distribution in the UPC (water piping, detail), ^{16}N.

4.1. Tritium permeation barriers

According to the location (e.g. in BB, TER and PHTS systems), the permeation barrier can be subjected to different conditions. For instance, when located within the BB, they are subjected to a very harsh environment with high neutron irradiation, while within the TER and PHTS, the conditions are more relaxed. Under the term "permeation barriers", it is possible to identify two different technological solutions: i) the alumina (Al_2O_3) coatings of the steel structures and ii) the chemical control of the oxides at the steel surface. Concerning the first

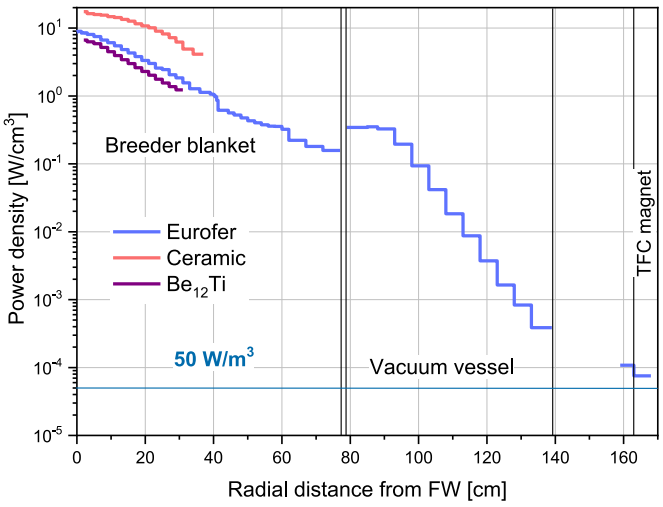

Fig. 8. Radial power density profiles for HCPB BB.

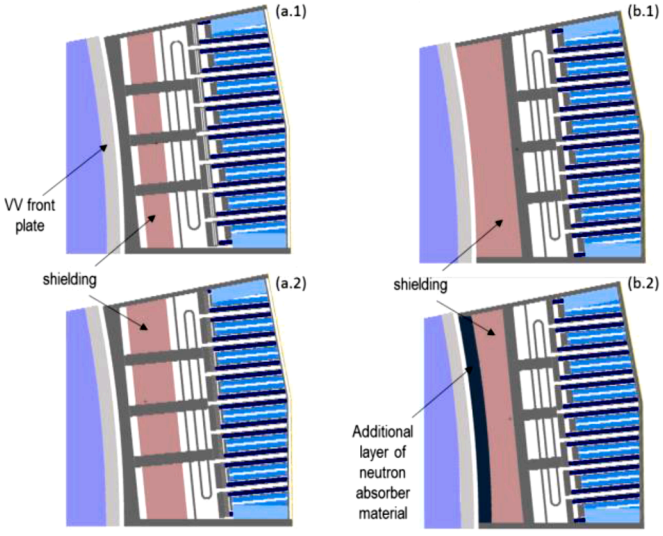

Fig. 9. IB HCPB layout with integrated neutron shield. Configurations (a.1) and (a.2) with internal shield of 12 cm and 18 cm, respectively (in-BSS). Configurations (b.1) and (b.2) with external shield of 18 cm and 12 cm + 6 cm absorber, respectively (behind BSS) [25].

type of T permeation barrier, three types of Al_2O_3-coatings have been developed to minimise the T permeation (they can have also the effect of limiting the corrosion or provide electrical insulation in PbLi flow for the WCLL concept). They were developed at a laboratory scale and a preliminary scale-up of the technologies was performed [26]. The technologies investigated are the Electrochemical process (ECX), Pulsed Laser Deposition (PLD) and Atomic Layer Deposition (ALD). These technologies have shown good performances in screening experiments.

Characterization tests have shown, namely:

- PLD: tested up to 650 °C with a Permeation Reduction Factor (PRF) up to 1000–10,000, good compatibility with PbLi (corrosion test carried out in stagnant PbLi), no modification of the coating after neutron irradiation in LVR-15 reactor and thermal cycling (1000 cycles with T_{min} equal to 100 °C, T_{max} equal to 450 °C and a ramp of 40 °C/h). Good electrical insulation properties have been verified after the previously mentioned tests and under ion irradiation. The coating can be manufactured at low temperature (~ 100 °C) only on the external surface of the components, therefore it is possible to coat WCLL water tubes and the internal surface of the FW.
- ALD: tested up to 550 °C with a PRF up to 900–1000, good compatibility with PbLi (corrosion test carried out in stagnant PbLi), after thermal cycling (500 cycles with T_{min} equal to 100 °C and T_{max} equal to 450 °C). Good insulation properties have been verified after the previously mentioned tests. The coating can be manufactured at low temperature on all surfaces (inside and outside BB or pipes).
- ECX: PRF up to 100–200, good compatibility with PbLi (corrosion test carried out in flowing PbLI up to 16.000 h). No modification of the coating after thermal cycling (2000 cycles) between ~300 and 550 °C has been observed. The coating can be manufactured on all surface (inside and outside BB or pipes) but is realized at high temperature (~ 980 C) and a further heat treatment would be required for EUROFER97.

In conclusion, three fabrications for Al_2O_3 coatings technologies have been developed successfully up to a semi-industrial scale. They show PRF able to reduce permeation at least 10 times more than what has been assumed in the past to determine the CPS requirements. However, their behaviour under neutron irradiation at relevant dpa has not been yet demonstrated. Experiments are still missing and would be necessary for the application to the BB. The applicability to an industrial scale also needs to be further assessed, namely their applicability to complex geometries and/or big components, as well as compatibility with the manufacturing process (e.g. the coating of welds and joints). Ageing effects over the entire lifetime in flowing liquid metal are not yet fully known.

Regarding the second type of permeation barrier, a possible control of coolant chemistry can be used to produce a weak form of T permeation barrier able to reduce the T permeation in the range of 10–100. This solution could be considered as an option for the design of the HCPB PHTS to avoid the necessity of a coating. The adding of small quantities of O and H in the helium flow can sustain a thin oxide layer on the steel, reducing the permeations (the "self-healing" effect, i.e. capability of repairing defects/cracks of the oxide layers, of oxidizing atmospheres with the presence of O_2 and water in He has been also observed/supposed in [27]). However, in this case the impact of adding impurities to helium to the erosion/ corrosion of steel pipes must be investigated. The evaluation of the performance of this system is based on old data [28] related to Inconel and MANET, however, an experimental confirmation for a transfer to EUROFER is lacking.

4.2. CPS variants and performances

Concerning the CPS to be equipped in a Water-cooled DEMO architecture, efforts have been dedicated to reviewing the existing large water detritiation facilities to understand the issues associated with the size, complexity and costs of such systems. Table 1 illustrates the main characteristics of some relevant water detritiation facilities around the world that have been developed for fusion and fission nuclear power plant. By taking into account the dimension and cost of the water detritiation facilities (see Table 2), the main achievements of the T Permeation Barrier (TPB) activities (Section 4.1) and the value of the maximum tritium concentration inside water coolant c_0 equal to 1.85E + 11 Bq/kg (5 Ci/kg[8]) (assumed after having reviewed the Canadian tritium experience [29, 30]), two solutions are currently proposed: (i) in-line CPS and (ii) off-line CPS. The first solution foresees the use of TPB. Required BB PRF is set to a modest value of 100 and a CPS in-line with the water primary coolant loop having the same dimension of the ITER Water Detritiation System (WDS) is selected. A by-pass of 20 kg/h

[8] This limit, derived by the tritium concentration in the heavy water of CANDU reactor, is far above the current limit used in ITER RPrS for water coolant that is equal to 0.11 GBq/kg (~0.003 Ci/kg).

Table 1
Main characteristics of some relevant water detritiation facilities.

Facility	Process	Feed stream, kg/h	Dimensions	Additional info
DTRF	VPCE+CD	360	The building is 35 m long, 25 m wide, 12 m height expected for the CD, 38 m height	In operation since 1987. Power input of the refrigerator unit 1550 Kw
WTFR	LPCE+CD	100	2 LPCE columns with a diameter of 0.6 m, the height of about 20 m each.	In operation since 2007. 55 catalyst sections with Sulzer CY packing
CTRF	LPCE+CD	40	3 LPCE columns and 4 CD columns	Under design, commissioning in 2024.
ITER WDS	CECE	20 (× 3)	LPCE column of 26 m height, electrolysis cell of 50 m3/h (120 kA)	Operation in 2027.
JET WDS	DE+CD	3.7 – 5.6	–	–
AREVA NC La Hague	WD	5000	13 columns each 4 m diameter, 25 m height packed with 1200 tons of copper	Tentative design. Two different options are proposed, both would consume about 150 MW and investment cost of about 1000 M€
	CECE		3 LPCE columns each 2 m diameter, 5.5 m height and 800 electrolysers each 30 m3 capacity	

Acronyms
DRTF = Darlington Tritium Removal Facility
WTFR = Wolsong Tritium Removal Facility
CTRF = Cernavoda Tritium Removal Facility
ITER WDS = ITER Water Detritiation System
JET WDS = JET Water Detritiation System
VPCE = vapor Phase Catalytic Exchange
CD = Cryogenic Distillation
LPCE = Liquid Phase Catalytic Exchange
CECE = Combined Electrolysis Catalytic Exchange
DE = Direct Electrolysis
WD = Water Distillation

Table 2
Sensitivity matrix for WCLL DEMO.

Parameter	WCLL Case-0	Min/Inter.	Max
CPS by-pass flow rate [kg/h]	0	20	360
TER efficiency [%]	82	80	95
T perm. rate from plasma [mg/d]	0	0	20
PRF in BB [-]	100	1	1000
H_2 concentration in water [ppm]	8	8	100
PRF in PbLi loop[-]	1	100	1000
H_2O leak rate from HXs [kg/h]	0	0.3	0.6

of water is continuously routed and processed inside the CPS. Also, the second solution foresees a PRF_{BB}=100 but in this case, the CPS is placed off-line the primary water circuit and, again, it has to process about 20 kg/h (same as ITER WDS). In practice with the second solution, the entire BB PHTS water coolant has to be discharged when the limit of 1.85E + 11 Bq/kg (5 Ci/kg) is reached, replacing with fresh water and processed in a dedicated WDS facility. Such a procedure is implemented also in the tritium displacement program used in CANDU for tritium recovery and heavy water purification [16]. Concerning the detritiation systems to be selected for water CPS, two processes (and also their combination) are currently considered: (i) the Water Distillation (WD) and (ii) the Combined Electrolysis Catalytic Exchange (CECE). Water distillation is a well-established technology for heavy water upgrade in CANDU reactors and can be promising if used as pre-concentration stage or for the case in which high decontamination efficiency is not mandatory (i.e. in the in-line CPS). Instead, the CECE combines an electrolyser and a Liquid Phase Catalytic Exchange (LPCE) column in which isotopic exchange between liquid water and hydrogen are promoted via hydrophobic catalyst. With CECE is possible to achieve high decontamination factor, thus it is a valuable option for an off-line CPS. Despite these considerations, during the conceptual design phase more accurate models will be implemented to better evaluate the described detritation systems [31,32].

Regarding the CPS to be equipped in a Helium-cooled DEMO architecture, it is composed of two main subsystems: one for removing the hydrogen isotopes and one for the removal of other impurities. For the removal of the hydrogen isotopes, two different options are proposed while the removal of the other impurities is always achieved by a combination of filters and non-regenerable getters for which the design can be improved only when information about the amount and the composition of such impurities becomes available. Regarding the removal of hydrogen isotopes, two different processes are proposed for the DEMO CPS helium-coolant: one is based on the scale-up of the "conventional" process used in fission and also in ITER CPS, and another relies on the use of novel NEGs material, Figs. 10 and 11 provide the layout of the two processes [33]. Among the main input data used to define the coolant by-pass inside the CPS, two are of particular interest: the tritium permeation rate from the blanket into the coolant ($F_{T,p}$) and the tritium concentration inside helium coolant (c_0). The c_0 strongly depend on the tritium removed by the CPS (i.e. efficiency, 80–95%) and on the tritium that permeates from the BZ to the coolant. According to a reference found in the literature related to ITER CPS [34], initially, an HT partial pressure in He-coolant of 4E-02 Pa was assumed. However, as reported in [35], some calculations performed in the past have demonstrated that 1 Pa of HT should be assumed as a threshold limit keeping tritium losses (i.e. T permeation rate through oxidized Incoloy 800 steam generator tubes) below 20 Ci/d. Therefore, the HT pressure of 1 Pa has been also included in the calculation. For the case in which the allowable tritium concentration in helium coolant is 1 Pa, the resulting coolant by-pass inside the CPS is 0.12 kg/s instead of 3 kg/s derived using an HT partial pressure in He-coolant of 4E-02 Pa. The last parameter that has an impact on the CPS design is the H_2 content inside the helium coolant. Besides the amount of hydrogen that permeates from BB and FW, some H_2 can be added to the coolant for reducing the Q_2 permeation from BB into coolant [36]. In this view, it is important to notice that the H_2 addition has a great impact on the size of the CPS technologies and on the time required between one regeneration and another, thus on the lifetime of several components. Particularly in the report [37], a preliminary dimensioning of main CPS technologies considered in the two design options (CuO beds and zeolite molecular sieve beds for the first option and NEGs for the second option) has been performed by assuming different values for the H_2 addition corresponding to 80, 300 and 1000 Pa, although the last value imposes severe working conditions to the CPS [15].

4.3. T permeation rates and inventories

The studies carried out aimed to provide a list of tritium inventories in the BB system and tritium chronic releases as per tritium permeation analyses for the DEMO 2017 baseline, taking into account both variants with water and helium. In this regard, the BB, TER CPS and PHTS systems have been considered focusing the attention on the interfaces as shown in Figs. 2 and 5. A T generation rate of 320.26 g/d (assuming 2 h pulse and 10 min dwell between the pulses), and the T permeation rate from the plasma (0–60 mg/d), have been taken into account as integral tritium sources.

To investigate the effect of the different system performances in terms of T management and to identify the impact on DEMO

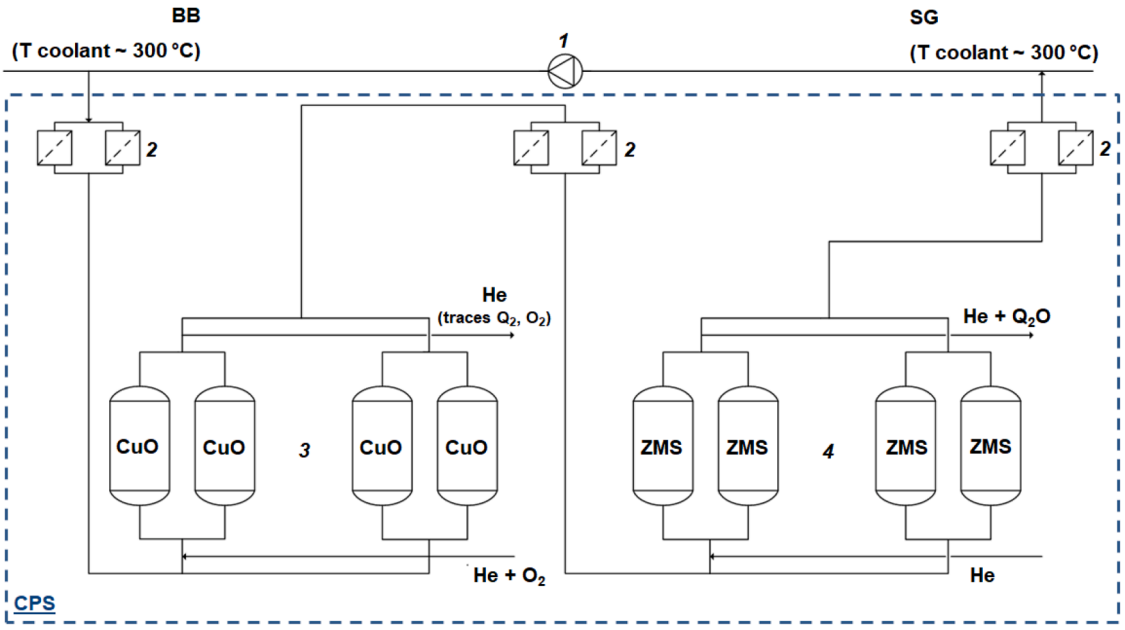

Fig. 10. DEMO CPS layout for He-coolant based on the scale-up of the ITER process.

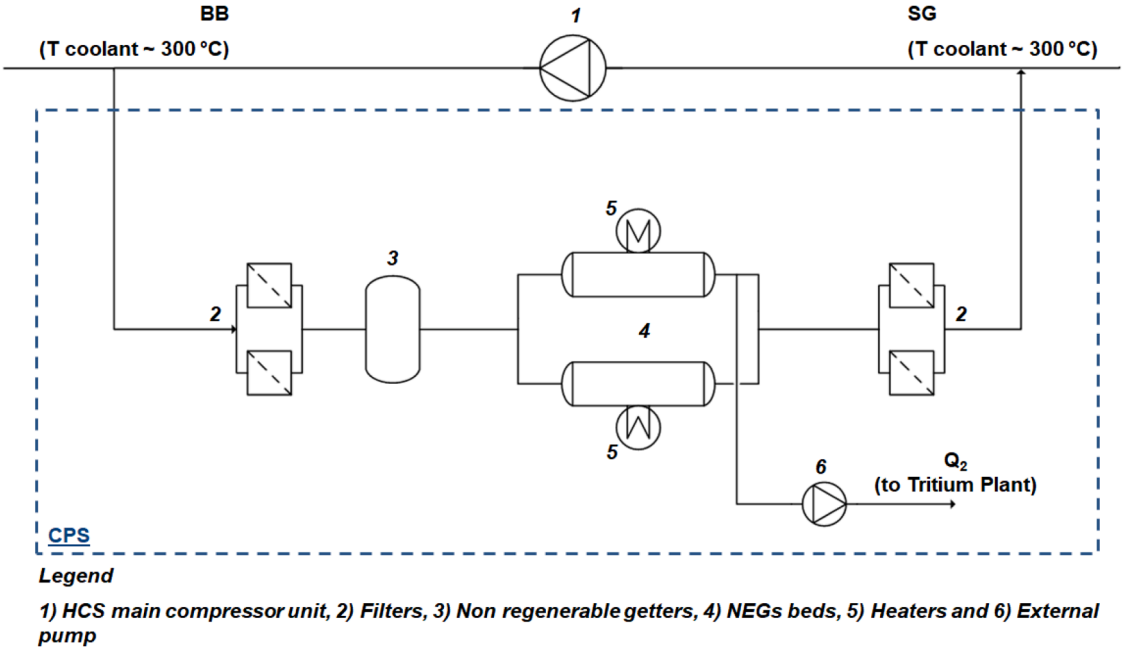

Fig. 11. DEMO CPS layout for He-coolant based on the use of NEG beds.

architecture in terms of inventories and releases, several parameters have been considered. Starting from these parameters, a sensitivity analysis has been performed using parametric studies according to the sensitivity matrix reported in Tables 2 and 3. Starting from the base-case scenario denoted as "Case 0", a parametric study has been performed relying on a one-at-a-time parameter modification. This list of parameters addresses the system performances (e.g. TER system extraction efficiency, CPS by-pass flow rate and permeation reduction factor) and operational figures (doping hydrogen pressure into the coolant, leak rates from primary to secondary system, etc.).

As a result, the minimum and maximum variations in inventories and releases that occur in each interfacing system involved in T management have been evaluated. The results are reported in Tables 4 and 5.

For WCLL, the studies have shown that the major contribution to the permeation losses comes from the PbLi ex-vessel piping. The high permeation surface added to the relative high tritium concentration in PbLi produces high permeation rates through the pipe walls to the room (~150 mg/d for Case 0). The releases into the Tokamak building can be reduced by increasing the TER T extraction efficiency (from 150 mg/d to ~69 mg/d) and using the permeation barriers (e.g. PRF 1000) on the PbLi loop (~0.15 mg/d). On the other hand, the chronic releases from the PHTS piping are negligible (between 10^{-14} and 10^{-12} g/d, see

Table 3
Sensitivity matrix for HCPB DEMO.

Parameter (unit)	HCPB Case-0	Min/ Inter.	Max
CPS by-pass flow rate [kg/s]	3	2	4
CPS efficiency [%]	90	80	95
H_2 part. Press. in helium coolant [Pa]	0	1	300
He purge gas flow rate [kg/s]	0.497	0.25	0.5
TER efficiency [%]	80	80	98
T perm. rate from plasma [mg/d]	3.5	0	60
He leak rate [%inventory/yr]	4	0	36.5
PRF on IHX pipes	100	1	1000
Steam conc. in purge gas [%]	0	0	4
He leak rate from HXs [kg/h]	0	0.024	0.34

Table 4
WCLL T inventories and permeation rates variation[1122334455].

WCLL Sensitivity Analyze	Case 0	Min	Max
Inventories in water [g]			
Blanket BZ	63.3	6.4	70.4
Blanket FW	1.0	0.6	5.8
PHTS BZ	63.5	6.4	70.7
PHTS FW	1.9	1.1	11.1
Inventories in steels [g]			
Blanket	3.4	2.9	3.5
PHTS BZ	4E-04	5E-05	1E-03
PHTS FW	8E-06	5E-06	5E-05
TER piping	2E-01	3E-03	2E-01
Inventories in PbLi [g]			
Blanket	35.1	30.0	36.0
TER	0.9	0.4	1.0
Permeation rates [mg/d]			
Through the BZ PHTS SG	0.18	0.02	0.7
Through the FW PHTS SG	0.02	0.01	0.09
Through BZ PHTS piping	0	0	0
Through FW PHTS piping	0	0	0
Through TER piping	152	0.15	170
From PbLi to BZ PHTS	420	42	432
From PbLi to FW PHTS	9.28	0.92	9.28
SG leak rate from BZ PHTS	–	41.7	67.1
SG leak rate from FW PHTS	–	2.07	3.19
Extraction rates [g/d]			
Extraction rate TER	304	304	306
Extraction rate CPS	–	0	0.41

Table 5
HCPB T inventories and permeation rates variation[61].

HCPB Sensitivity Analyze	Case 0	Min	Max
Inventories in helium [g]			
Blanket coolant	1E-02	1E-03	1E-02
PHTS	1E-02	2E-03	2E-02
Blanket purge gas	6E-02	3E-02	1E-01
TER purge gas	1E-01	7E-02	2E-01
Inventories in steels [g]			
Blanket	2E-02	3E-03	4E-02
PHTS	4E-01	5E-02	1.1
TER piping	8E-02	4E-03	0.2
Inventories in Breeder and Multiplier [g]			
Ceramic Pebbles	24.5	24.5	24.5
Neutron Multiplier	71.8	71.8	71.8
Permeation rates [mg/d]			
From purge gas to PHTS	365	61.5	738
Through TER piping	11.5	0.55	23.7
Through PHTS IHX	0.58	0.06	52.2
Through PHTS piping	6.28	0.78	15.4
PHTS leak rate	0.002	0	0.015
IHX leak rate	–	0	0.001
Extraction rates [g/d]			
Extraction rate TER	310.1	309.5	310.5
Extraction rate CPS	0.36	0.1	0.7

Table 4). In terms of T inventories, moderate variations (~18%) in the blanket steel (see Table 4) occur changing the operating parameters of the different systems and a negligible amount is trapped within the piping of PHTS and TER.

However, strong variations have been encountered within the water according to the performances of the CPS. Indeed, as shown in Table 4, the T inventory in water the BZ BB and BZ PHTS can decrease from ~140 g to ~13 g increasing the CPS by-pass flow rate from 0 kg/h (Case 0 with off-line CPS) to 360 kg/h (same mass flow rate used in the existing DTRF facility [38], see also Table 1). The high T inventory in water implies significant losses associated with the water leaks in the SGs. Both the permeation barriers in the blanket and the action of a CPS would importantly reduce these losses.

For HCPB, the major contribution to the T releases comes from the permeation rate through the TER piping (~11.5 mg/d for Case 0) due to the high permeation surface added to the relative high tritium concentration in the purge gas.

These releases can be reduced by increasing the TER T extraction efficiency up to 98% (~9 mg/d) or using steam as doping gas in the purge gas (~0.55 mg/d). For the HCPB blanket, a crucial role is played by permeation reduction on the IHX pipes, achieved, for instance, by controlled oxidation [39]. Mitigating the parasitic losses due to permeation is essential in He-cooled blankets to comply with the safety limits. It is interesting to note that very high leak rates from the PHTS to the building (e.g. 36.5% of the coolant inventory per year) do not play an important role in terms of T releases since the T inventory present in the helium coolant is very low (between 3 and 0.3 mg, see Table 5). In terms of T inventories, they are quite low in the BB, PHTS and TER piping steel (see Table 5). However, a considerable amount of T is trapped within the ceramic breeder (~24.5 g) and in the neutron multiplier (~71 g) in 5 fpy. In particular, the beryllides blocks have been modelled taking into account the experimental results in terms of T production (~1.33% of the T generation in the ceramic breeder) and retention (lower than 1% after 470 °C, $T_{ave\_Be12Ti} \approx 696$ °C) according to [40, 41].

For both BB concepts, it is worth noting that a high amount of T is trapped into the FW and, in particular, in the tungsten armour due to the tritium implantation from the plasma. Indeed, hundreds of grams of T are trapped within the tungsten posing serious issues in terms of (i) starting inventory necessary to saturate the structures, (ii) confinement of T during remote maintenance of the BB and (iii) management of tritiated waste at the end-of-life of the BB. More info can be found in [42].

4.4. Fuel cycle and required and target TBR

DEMO must produce sufficient tritium to guarantee its planned operational life and start-up another Fusion Power Plant. This goal is enshrined in the doubling time t_d, which is the time required to breed enough tritium such that an amount of tritium equal to the start-up inventory $m_{t,start}$ of the plant can be delivered without impacting operation. This start-up inventory is dependent on a multitude of parameters, most notably the fuel cycle operational inventory, the amount of tritium retained during operation, the tritium breeding ratio as well as the achievable plasma availability and burn-up fraction. Of these, the amount of tritium retained in the first wall differs most notably between the BB options, due to the different operating temperatures of the first wall. Dedicated studies of this effect are presented in [42,43] and tentative values of 625 and 350 g have been used as T inventories for WCLL and HCPB, respectively. A simplified dynamic fuel cycle model was developed (see [44]) that can estimate the start-up inventory and reactor doubling time for a given design point, taking into account the effects of tritium sequestration in a range of sub-systems. Reduced models of tritium trapping in the first wall were developed to mimic the effects shown in [42]. For the EU-DEMO reference design point (a fuel cycle operational inventory of 2 kg [45], a TBR of 1.05, and an assumed

Table 6
Start-up inventory and doubling times for the reference case of both blanket scenarios [42].

	$m_{t,start}$ [kg]	t_{double} [calendar years]
HCPB	2.84	5.33
WCLL	2.99	6.26

full power plasma availability of 30% [42]) the start-up inventories and doubling times as given in Table 6 were obtained.

The doubling time is reasonably fast in both cases, within less than half the expected total plant lifetime. If longer doubling times are permissible, the TBR requirement can be relaxed, especially at later stages of the plant lifetime once components are saturated and higher availabilities are expected. On the other hand, the BB has to demonstrate the technical maturity and feasibility of the technological solutions used to fulfil the main design requirements: sufficient tritium production and reliable energy generation. The former implies tritium breeding per one plasma source neutron, i.e. TBR, in an amount exceeding the fixed design target (e.g. 1.03–1.05) by a certain value ΔTBR. This TBR excess accounts for uncertainties coming from diverse assumptions made in the DEMO project to enable the blanket development without inclusions of not well-known features and not enough elaborated sophisticated engineering solutions. One of the most significant simplifications adopted in the BB developments is a neglect of the necessary cut-outs for adopting various in-vessel components (IVC) in the tokamak design, such as limiters and openings for particle injection into the plasma. It means that the particular blanket design permits the application of various simplifications negatively affecting the TBR, assuming that the tritium breeding capability of the blanket compensates for these effects. Therefore, a study was performed to enable a parametric and modular assessment of the TBR accounting for diverse possible openings in the blankets for an arrangement of the IVCs. The neutronic analyses aim at building a catalogue, i.e. providing for each auxiliary system and the corresponding cut-outs the expected TBR impact [46]. The proper functioning of the DEMO fusion reactor is maintained and controlled through auxiliary (not tritium breeding) systems arranged in the tokamak. The main purposes of these systems are the protection of the blanket against plasma disruptions, feeding of the plasma volume with neutral deuterium and tritium atoms, plasma heating, plasma diagnostic and supporting the plasma stability. Due to physical and technical requirements, these systems are supposed to be toroidally distributed in the tokamak chamber to fulfil the project requirements. A 360° neutronic model of DEMO was realized including the following IVCs (see also Fig. 12):

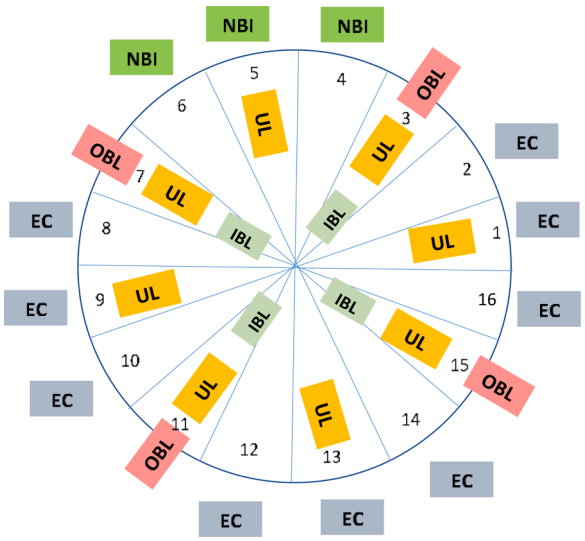

Fig. 12. IVCs arrangement in DEMO [46].

- 4 inboard mid-plane limiter (IBL),
- 4 outboard mid-plane limiter (OBL),
- 8 upper port limiter (UPL),
- 4 lower mid-plane limiter,
- 3 Neutral Beam Injector (NBI) systems,
- 9 Electron cyclotron (EC) antennas (representing also diagnostic port plugs which no design is available so far).

The TBR calculations were performed with the MCNP code making use of all geometry models for different IVC integrations. The separate effect of the TBR due to various IVCs was assessed comparing the results with a full BB model (i.e. without any cut-outs). It has been found that the TBR decrease due to the allocation of all IVCs is 11%. This means that depending on the TBR_{req} value adopted in the DEMO project (assumed range being 1.03–1.05) the target TBR, $TBR_{target,}$ can vary from 1.14 to 1.17, accounting for the impact of the integration of the IVCs [46].

5. Impact of BB variants on safety

The selection of the BB concept affects also the design of safety systems.. Indeed, due to the different coolants, inventories and enthalpies in the BB, the solutions to be adopted for the mitigation of accidental scenarios can be different. This is the case of the Vacuum Vessel Pressure Suppression System (VVPSS) that is designed to protect the DEMO VV and attached components from overpressure conditions in the case of an incident or accident and to retain the radioactive inventory which could be mobilized after an In-Vessel Loss Of Coolant Accident (LOCA). The VVPSS shall be available at any time there is a possibility of overpressure to the VV. This situation could arise during periods of normal operation evolving in an incident or accident. In the following paragraphs, an overview of the main functions, requirements and design solution both for the Water and Helium-cooled DEMO architectures is reported.

5.1. VVPSS configuration

The first safety function of the VVPSS is to confine the source terms in case of an incident/accident. Furthermore, the VVPSS, as part of the first confinement barrier should be classified as a safety system. However, the safety classification of the VV and its extension has not been assessed yet but it is straightforward that, being part of the first confinement, it is a SIC-1 (Safety Importance Class 1) component. The primary VVPSS functions identified so far are:

[6] The *T* inventories due to the permeation from the plasma (e.g. ~700 [g] [31] considering that the full flux from the plasma is T. Assuming that a half of the flux is composed by Deutirium, the value to be considered is ~ 350 g) should be added on top of the inventory in HCPB BB steel calculated in T permeation analyses.

[2] These values are taken at different time when an operational limit is overcome. In particular, the minimum is reached at 5 fpy assuming the maximum CPS by-pass flow rate (see Table 2) while the maximum is obtained after 0.85 fpy assuming 100 ppm of H_2 in the PHTS water.

[3] The values refer to different cases. The minimum is calculated after 5 fpy for the case with PRF in BB of 1000. The maximum is assessed after 5 fpy for the case without CPS.

[4] The maximum permeation rates corresponds to the reference PRF = 100. The PRF = 1 scenario implies unacceptable permeation rates (~10^2 g/day).

[5] The leak rates are calculated after ~0.86 fpy.

[6] The *T* inventories due to the permeation from the plasma (e.g. ~700 [g] [31] considering that the full flux from the plasma is T. Assuming that a half of the flux is composed by Deutirium, the value to be considered is ~ 350 g) should be added on top of the inventory in HCPB BB steel calculated in T permeation analyses.

- To protect the VV from overpressure keeping the maximum pressure inside the VV below 0.2 MPa absolute in case of in-vessel LOCA (the pressure limit is imposed by the auxiliaries' penetrations, e.g. diamond windows).
- To assure the leak tightness of the expansion tank.
- To retain its structural integrity.
- To mitigate hydrogen explosion risk by
  - Collection of hydrogen in a sealed volume of VVPSS tank.
  - Reduction of hydrogen concentration to below 1% in gas to be discharged to the Detritiation System (DS).
  - Monitoring hydrogen concentration online in the gas flow to be discharged to DS.
  - Processing hydrogen accumulated in the sealed tank of VVPSS during post-accident operation.

The system includes large Expansion Tanks (ETs) containing enough water at a temperature $\leq$ 40 °C and low pressure to condense the steam or to suppress the pressure resulting from the most adverse In-Vessel coolant leaks into the VV, thus limiting over-pressurization to 0.2 MPa absolute. The system can also be utilized in a variety of other situations, such as a simple loss of vacuum, to provide overpressure protection and enhanced confinement by maintaining low pressure in the system. The ETs are connected through piping which is routed from the VV plasma chamber. These relief pipes incorporate Rupture Disks (RDs) system that is put in parallel for redundancy. This system is designed to rupture/burst when a severe Ingress of Coolant Event (ICE) or other postulated overpressure incident or accident occurs. The main function of the VVPSS is passive and provided by the RDs. The primary RD is the main vacuum confinement boundary in normal operating conditions. When ruptured, this disk assembly allows direct connection of the VV to the VVPSS ET. This is envisioned to occur in only the most severe event Categories. The system design also includes redundant bypass lines (Bleed Lines, BLs) in parallel to the rupture disk system equipped with Bleed Valves (BVs) that will intervene at lower VV pressure (0.9 bar) with respect to the RD (e.g. 1.5 bar). They control less significant events (small leakages) avoiding in some case the intervention of RD while providing a negligible contribution to the pressure suppression in case of larger LOCAs. Fig. 13 illustrates schematically the functionality of the VVPSS.

In DEMO, the in-vessel available volume for containing primary coolant in case of a leak is ~6260 m^3. It is subdivided among (see Fig. 14):

- Upper port – Large ring manifold volume ~1664 m^3;

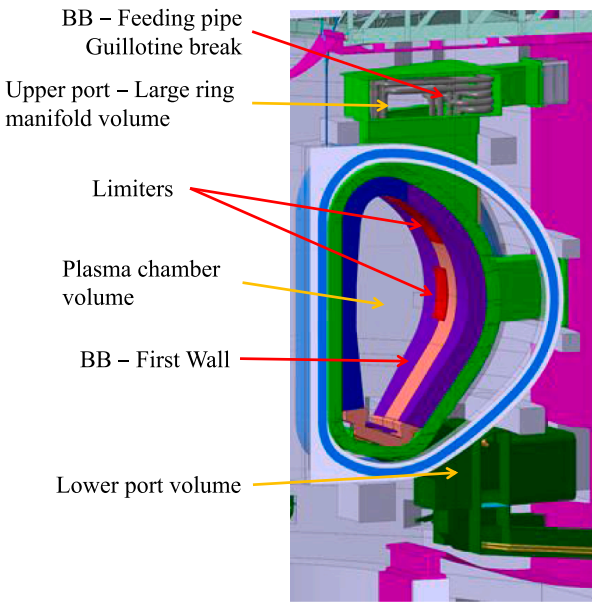

Fig. 14. In-Vessel volumes and leak sources.

- Plasma chamber volume ~2964 m^3;
- Lower port volume ~1630 m^3.

Being the VVPSS one of the most important passive safety systems to be foreseen in the DEMO plant, design and integration challenges have to be faced to ensure that best performance within safety requirements are always achieved. For this purpose, an accidental sequence has been selected and analyses have been performed to support VVPSS design and integration activities. For both WCLL and HCPB concepts, the selected postulated initiating event is the failure (guillotine break) of the BB collector pipe located inside the upper port. As a consequence of it, an unmitigated disruption may occur. In DEMO, limiters are designed to protect the BB FW in case of disruption. Two accident sequences have been studied. For the baseline accident used to dimension the VVPSS, it is assumed here that the limiters fulfil their function and terminate the plasma. The sizing analyses are also carried out for the worst-case scenario, in which the limiters fail and thus the FW damaged as a consequence of the disruption. The two accidental scenarios are:

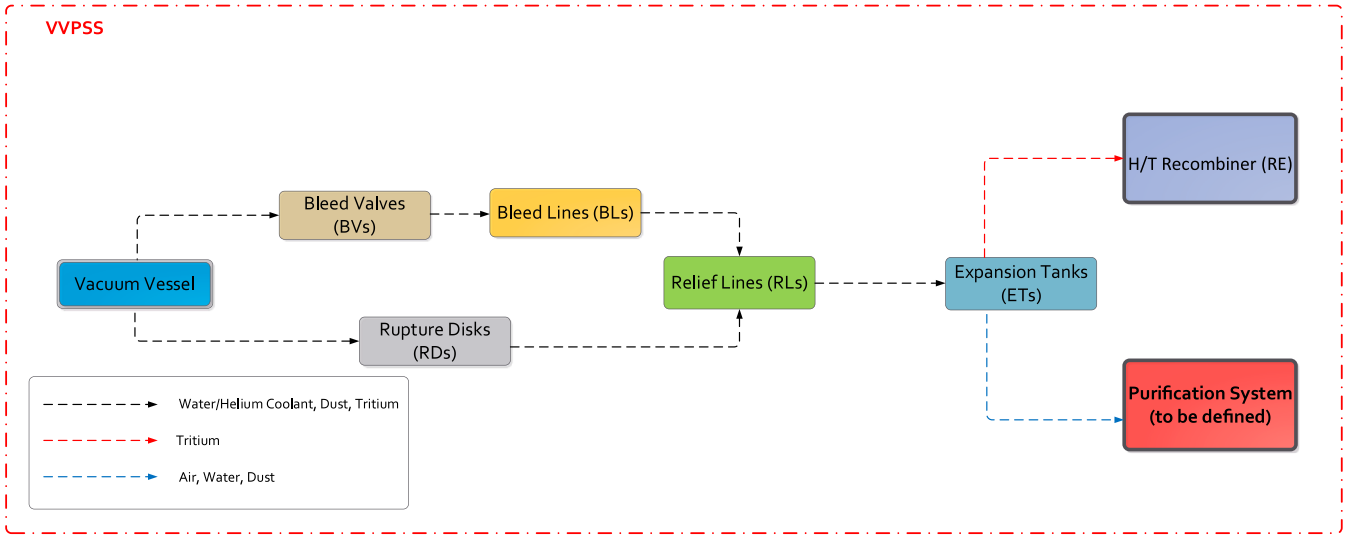

Fig. 13. Schematic drawing of the VVPSS.

- Worst accidental scenario:
  - For the Water-cooled DEMO architecture, the Double-Ended Guillotine (DEG) break in the hot leg of WCLL BZ-PHTS produces an unmitigated disruption that affects 1 m^2 FW producing In-VV LOCA from the FW loop.
  - For the Helium-cooled DEMO architecture, the DEG break in the hot leg of one loop of HCPB PHTS induces an unmitigated disruption that, destroying 1 m^2 of FW, produces an In-VV leak from 2 additional PHTS loops.
- "Baseline" accidental scenario
  - For the Water-cooled DEMO architecture, DEG rupture in the hot leg of WCLL BZ-PHTS is assumed.
  - For the Helium-cooled DEMO architecture, the DEG rupture in the hot leg of one loop of HCPB PHTS is envisaged.

Furthermore, in case of a pipe break in the upper port region, there will be a local dynamic pressure peak from the jet of coolant onto the upper port walls and a distributed pressure peak due to the discharged coolant inventory. However, in the case of an In-Vessel leak, the local dynamic load from the jet of coolant will be on the neighbouring In-Vessel components. In this case, it has been demonstrated that the pressure on the point opposite to the leak inlet, reaches the largest value, steadily around the 2 bar limit imposed by the diamond windows. More detail about the 1D/3D CFD models that have been developed to assess the coolant dynamic behaviour in the case of LOCA and the results are reported in [47]. It has been assumed that the FW fails if the temperature reached by the EUROFER is higher than 1000 °C. Here the surface of 1 m^2 has been supposed to affect two segments belonging to two contiguous BB sectors served by different PHTS loops. The number of failed pipes below the surface has to be calculated accordingly for the HCPB and WCLL. The inventory lost by the HCPB and WCLL in case of a feeding pipe break or FW leak is summarized in Table 7.

To mitigate the overpressure in the VV, the BLs open when the VV pressure exceeds 0.09 MPa and the RDs when the VV pressure exceeds 0.15 MPa. The number of RD lines to be used to keep the pressure of the VV below the design pressure of 2 bar is determined by parametric analyses. If the pressure in the VV is above 80% of the design pressure the number of RDs is increased.

5.2. Sensitivity studies on VVPSS for water-cooled demo variant

Preliminary analyses for the baseline and worst-case scenario have been performed to determine the number of rupture disks, the volume of the tanks and the amount of water in the VVPSS necessary to suppress the pressure wave. The preliminary results, reported in Table 8, show that 5 or 6 ETs with a volume of 500 m^3 (filled with 300 m^3 of subcooled water) and a similar number of RDs are required for the baseline and worst-case scenarios, respectively. The peak pressure within the VV reaches 1.75 bar and 1.84 bar while the ET equilibrium pressure is 1.5 bar in both cases.

Further investigations have been conducted including the presence of Isolation Valves (IVs) in the WCLL PHTS with the scope to reduce the released coolant inventory during an In-Vessel LOCA and, therefore, minimise the peaks and the volumes of the ETs [48]. The IVs have been placed on the hot/cold legs and manifolds of the PHTS (see Fig. 15). IVs are effective in keeping a large quantity of the coolant inside the PHTS when placed on manifolds. Moreover, the strong equilibrium pressure reduction may lead to a lower space requirement for the VVPSS tank. Furthermore, they have a positive effect on the VV peak pressure and water inventory reduction (see Table 9). However, the use of IVs on the PHTS should be limited and if possible avoided. Indeed, having an active role during the accident in the minimization of the peak pressure and water inventory, they perform an important safety function. This means that they have to be redundant (i.e. high number of valves) increasing the complexity of the integration in the PHTS. Furthermore, the presence of IVs introduce a new initiating event (e.g. Loss Of Flow Accident, LOFA, due to the spurious closure of a valve) to be studied in safety analyses. Furthermore, being installed on the PHTS, as shown in Section 3.1, the IVs are subjected to neutron and gamma irradiation due to the ^{16}N and ^{17}N. Therefore, additional shielding has to be foreseen around the valve actuators to reduce the dose rate under 2 MGy posing further integration issues. Finally, in particular, for the IVs installed on hot/cold legs, the size poses manufacturability issues due to its dimensions. The same effect, in terms of reduction of the released water inventory, can be obtained by increasing the number of FW and BZ PHTS loops.

Furthermore, parametric accident analyses of an In-Vessel LOCA have been performed in [49] to determine the minimum flow area of VVPSS rupture disk pipes needed to maintain VV pressure below 2 bar. The parametric study includes 11 simulations performed by varying the rupture discs flow area for both baseline and worst-case accident scenarios. For the baseline scenario, considering the lower water inventory released within the VV (i.e. only the BZ PHTS water inventory is considered), the rupture discs line flow area required to withstand the safety-imposed pressure limit is 1.3 m^2, resulting in a total area of 7.1 m^2 as shown in Fig. 16. In addition to the substantial VV pressurization, steam injection into the plasma chamber causes the formation of hydrogen by the exothermic reaction between the steam and hot tungsten walls, releasing 156 kJ/mol according to the equation

$$W + 3H_2O \rightarrow 3H_2 + WO_3 \quad (1)$$

The total mass of hydrogen, calculated using MELCOR code, produced at the end of the simulation is 34.1 g. This mass adds to the 607.0 g of initial tritium. After 32 h from the Postulated Initiating Event (PIE), 19.3 g of hydrogen remain inside the VV; 626.3 g are collected in the VVPSS atmosphere. In particular, 221.8 g are collected in ET connected with the bleed lines and the remaining 404.5 g are equally distributed in the 5 ETs [49].

For the worst-case scenario, the very large releases of water and steam lead to rapid pressurization of the upper port and the plasma volumes. The maximum pressure reached in the VV volumes depends on the total flow area available for the discharge of steam in the VVPSS suppression tanks. Pressure increases very quickly and reaches the first pressure peak of 1.5 bar at about 1.958 s when the rupture discs open a path between the upper port and the suppression tanks. The timing of this peak is slightly influenced by the discharge area. Once the disks have ruptured pressure inside the VV continue to increase, because the total mass entering the VVPSS is lower than the mass entering the VV (Fig. 17) [49]. The worst-case transient results show that, to maintain vacuum vessel pressure below 2 bar, a total relief flow area of 8.6 m^2 is required. In the design, this flow area will be provided by 5 RDs relief pipes (draining steam in related suppression tanks) and by 6 bleed lines.

The total mass of hydrogen inside the VVPSS ranges between 471.0 and 520.3 g while the one remaining in the VV ranges between 101 and 150 g. Considering that the initial mass of hydrogen was set to 607.0 g (to take into account the initial mass of tritium inside the VV) the total mass of hydrogen produced ranges between 14.05 and 14.19 g [49].

Table 7
Coolant inventory lost for HCPB and WCLL in case of feeding pipe and FW break.[71].

Scenario	Description	Cause	PHTS inventory
Baseline	Feeding pipe guillotine break	Fabrication flaw	He: 215.5 m^3 - 1 PHTS H_2O: 326 m^3 - BZ PHTS
Worst case (additional wrt baseline)	208(He)/262(H_2O) FW channels	Plasma impact	He: 431 m^3 - 2 PHTS H_2O:127.2 m^3 - FW PHTS

Table 8
Preliminary results of VVPSS for Water-cooled DEMO architecture.

Scenario	Discharging Area [m^2]	Inventory involved [m^3]	VVPSS tank volume [m^3]	In-VV Peak pressure [bar]	Peak pressure timing [s]	Tank equilibrium pressure [bar]	# RDs
Baseline	0.0308	326	5 × 500, incl. 1 × 300	1.75	43.1	1.5	5
Worst case	0.0308 + 0.0257	326 + 128	6 × 500, incl.1 × 300	1.84	44.2	1.5	6

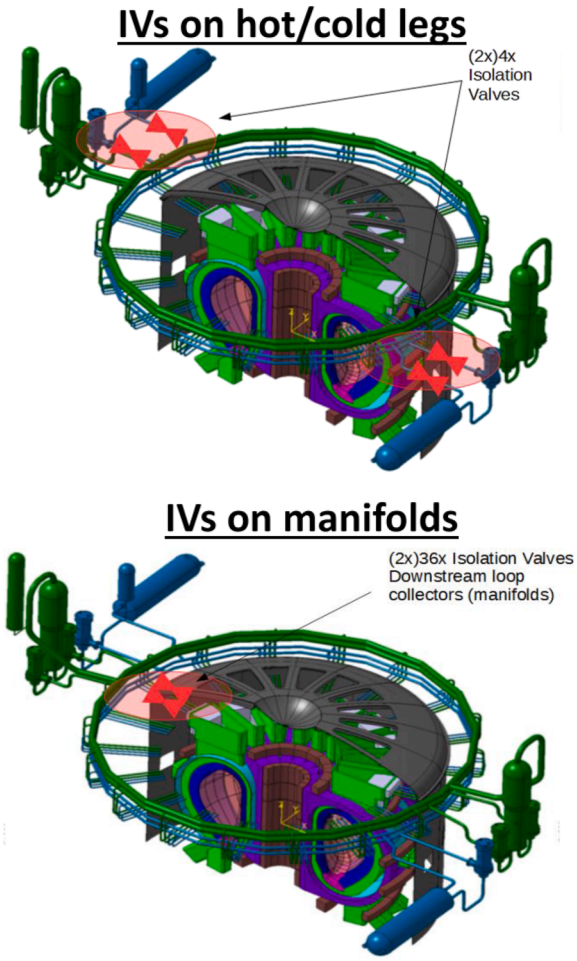

Fig. 15. IVs possible positions on the WCLL PHTS [48].

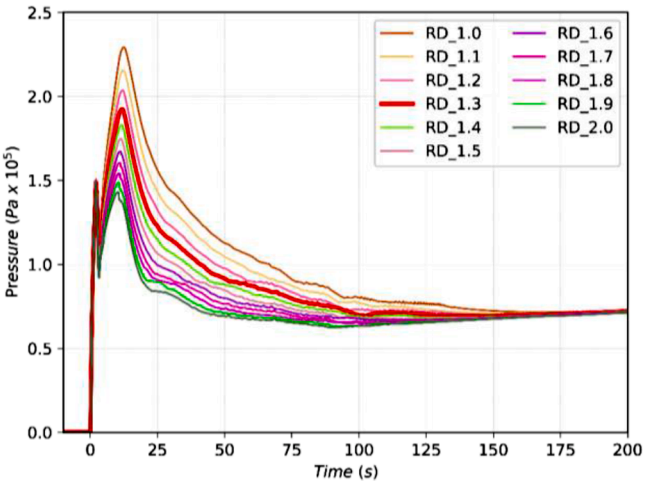

Fig. 16. Upper port pressure for different rupture disks flows area (baseline scenario).

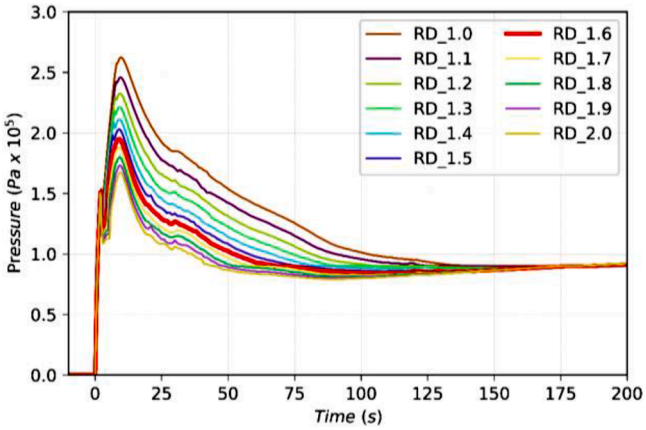

Fig. 17. Upper port pressure for different rupture disks flows area (worst case scenario).

Table 9
Effect of IVs in case of WCLL in the reduction of primary coolant inventory released, for the baseline scenario [48].

		IVs on manifolds	IVs on hot/cold legs
Valve closure time [s]		2	2
In–VV Peak pressure [bar]		1.69	1.70
VVPSS Equilibrium Pressure [bar]		0.495	1.25
Inventory reduction outside [%]	PHTS	78%	65%
	PHTS+VV	77%	65%
Maximum possible ET volume reduction [%]		86%	74%

[7] = the # of channels in case of 1 m^2 of EUROFER melted on the BB FW

5.3. Sensitivity studies on VVPSS for Helium-cooled demo variant

Analyses to support the design and the integration of VVPSS have been performed also for the EU DEMO HCPB concept. The preliminary results, reported in Table 10, show that:

- for the baseline scenario, 3 ETs of 1000 m^3 plus 1 of 1000 m^3 filled with 4% of water are required. In this case, the peak pressure reached within the VV is about 1.51 bar while 1.44 bar is reached at the equilibrium within the ETs.
- for the worst-case scenario, 3 ETs of 4500 m^3 plus 1 of 3000 m^3 filled with 5% of water are required. In this case, the peak pressure reached within the VV is about 1.9 bar while 1.67 bar is reached at the equilibrium within the ETs.

Table 10
Preliminary results of VVPSS for Helium-cooled DEMO architecture.

Scenario	Discharging Area [m^2]	Inventory involved [m^3]	VVPSS tank volume [m^3]	In-VV Peak pressure [bar]	Peak pressure timing [s]	Tank equilibrium pressure [bar]	# RDs
Baseline	0.161	215.5	3 × 1000 + 1 × 1000 (4% H2O)	1.51	1.64	1.44	3
Worst case	0.161 + 0.065	215.5 + 431	3 × 4500 + 1 × 3000 (5% H2O)	1.90	1.82	1.67	3

Also for the Helium-cooled DEMO architecture, a study on the application of the IVs has been performed. However, considering that in the case of In-Vessel LOCA, the pressure transient is too fast with helium (peak of pressure between ~1.6 and ~1.8 s, see Table 10), the effectiveness of the IVs to reduce the released inventory is negligible due to the time required by the IVs to close (usually ~2 s), and to the time required to detect the initiating event (3 s) [48].

Furthermore, two scenarios have been studied: the first foresees a dry expansion volume while for the second one the VVPSS is equipped with an in-pool heat exchanger emulating the Isolation Condenser (IC) installed in some Boiling Water Reactor (BWR) designs. In particular, for the first scenario, it has been considered to have 5 identical ETs of ~980 m^3 connected to the VV by means of 5 relief lines with a discharge area of 1 m^2 and an equal number of bleed lines which section is 0.05m^2; whereas for the second scenario, two of the previously considered tanks were used as a water reservoir (Pool) which host the Heat eXchanger (HX) connected to the remaining tanks acting as expansion volume. The main goal is to assess the pressure behaviour in the VV considering the design limit value of 2 bar [50].

The pressure-time evolution into the considered BB-PHTS loops and the VV is shown in Fig. 20 for both scenarios. The break occurrence is assumed at t = 0 s and a time delay of 3 s is assumed to shut down the plasma and starting with the decay heat simulation. The BVs open at 0.9 s since the differential pressure of 0.09 MPa is reached, while the RDs opening occurs at around 1.5 s when the 0.15 MPa set point is achieved. As can be seen, for the simulated conditions the VV exceeds the design limit of 0.2 MPa. Indeed, the pressure reaches the maximum value of 0.2603 MPa at around 15 s from the break opening, then it goes down at the equilibrium value of ~0.2312 MPa [50]. To comply with the pressure design limit of 0.2 MPa, the possibility to cool down the helium before coming to the ETs has been preliminarily investigated. In this way, the needed volume for its expansion can be reduced to an acceptable pressure. To that end, an IC-like solution has been considered instead of mixing directly helium with cold water to avoid the contamination (with tritium, activated corrosion products and dust) of the latter, since the limited capability of a potential detritiation system would require a long time to process it [50]. At the base of the analysed configuration, there is an HX immersed in a pool containing water at room temperature. The HX inlet is directly connected to the VV employing both relief and bleed lines, while the outlet is attached to the ETs (Fig. 18).

As concerns the HX design, the computational procedure has been based on the methodology reported in [51]. Starting from preliminary RELAP5–3D calculations the thermal power to be exchanged has been assessed to ~150 MW, then both the internal and external side heat transfer coefficient have been calculated.

The HX assessment has been done assuming the pool water

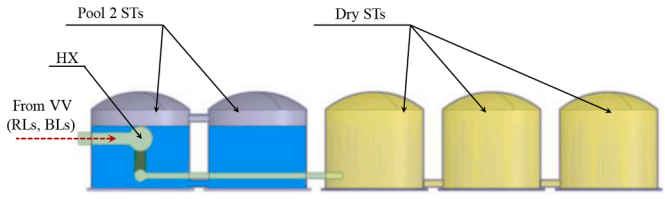

Fig. 18. HCPB VVPSS configuration with an immersed HX.

Table 11
HX main data.

Parameter	Value
Tube outer diameter [mm]	50.80
Tube inner diameter [mm]	48.80
Tube thickness [mm]	1.00
Design pressure [MPa]	0.25
Thermal conductivity [W/m•K]	20.34
Thermal power [MW]	150.00
Tubes length [m]	6.04
Number of tubes [-]	7821

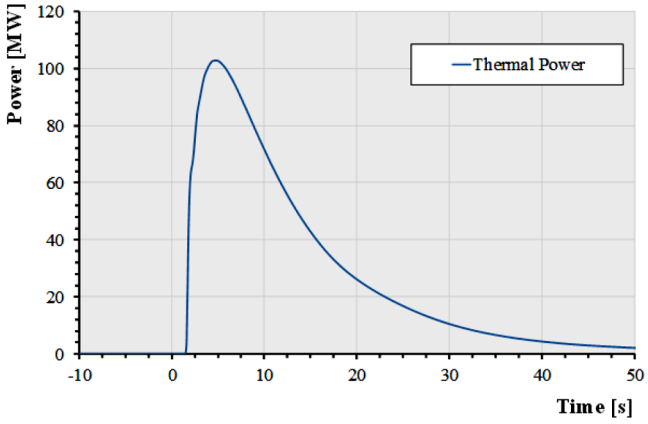

Fig. 19. Thermal power released into the pool water [50].

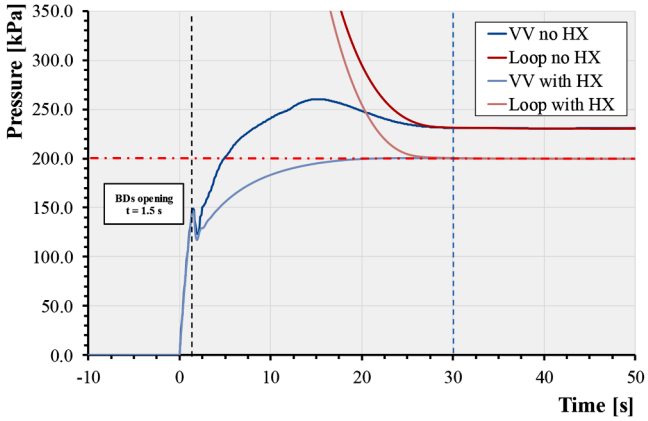

Fig. 20. VV pressure comparison [50].

temperature at 303.15 K, while the helium inlet and outlet temperatures have been iteratively obtained from RELAP5–3D calculations. The main HX information is summarized in Table 11 [50].

The HX, when triggered by the RDs opening, allows to cool down the helium up to ~150 °C thanks to the heat transferred to the pool water as depicted in Fig. 19. This effect works positively to reduce both the peak and equilibrium pressure values.

The VV pressure obtained for the analyzed configuration is reported, in Fig. 20, in comparison with that previously calculated.

As it can be deduced, the adopted solution is really promising as it allows us to reach a peak pressure slightly below the prescribed 0.2 MPa. However, the VV equilibrium pressure, being 0.198 MPa, basically lies on the design limit suggesting the need for further enhancement to safely stay underneath the limit. Some possible solutions may be the adoption of a greater expansion volume or adopting a different HX configuration, but both require additional feasibility studies which will be assessed in future work [50].

6. Lesson learned and further works

The selection of the BB variants will affect the whole configuration of DEMO in terms of radiation protection, tritium management and safety. In this paper, some of these aspects have been treated reporting the lessons learned during the Pre-Concept Design Phase and identifying the next steps to be followed to overcome the remaining issues.

In particular, concerning the issues related to the water activation, the results have shown that the dose rate values in the valve are very close or greater than the failure threshold value (2 MGy), considering a life of 6,7 fpy for the blanket. Results obtained show that the main contribution to the absorbed dose by matter in the UPC comes from the decay of ^{16}N decay and that, it is necessary to develop PHTS design changes to lower the dose absorbed by the valve. Some simple modifications (implying the use of bulkheads and/or Lead boxes) to shield the valve were studied in [20,21] to clarify the phenomenology under investigation. The data acquired in this work allow drawing some general considerations on the problem. Indeed, the complexity of the current PHTS design together with the dose rate levels calculated in the UPC suggest that solutions previously considered are not feasible due to the lack of space. Probably, the best way to ensure the availability of the valve throughout the blanket life is to reduce the water residence time in the zones subjected to intense neutron irradiation as well as increasing it outside the VV to reduce the ^{16}N and ^{17}N activity. Moreover, a benchmark activity is also planned with ITER results to check the developed analysis approach and to provide support to ITER Organisation.

Regarding the improvements of HCPB BB shielding performance to mitigate the activation of the VV, some progress has been made from a neutronic point of view. Indeed, it has been demonstrated that the use of a shielding material based on hydrate compounds of titanium, yttrium and zirconium is effective. Furthermore, it has been found that the same level of damage accumulation in the vacuum vessel in the mid-plane of the inboard side can be achieved utilizing between 12 and 18 cm of TiH_2, $ZrH_{1.6}$ or $YH_{1.75}$ and arranged in the BSS or outside of the blanket. However, additional studies are needed during the period 2021–2025. These should be focused on (i) the mitigation of the TBR reduction by applying the variable thickness of the shield along with the poloidal position in the blanket BSS, (ii) the investigation of the tritium retention and the temperature control within the shielding material, and (iii) the determination of the manufacturing procedure to be followed for its integration.

On the permeation barriers, the performances of the three depositing technologies are promising in terms of PRF (e.g. between 100 and 1000). These performances have been also tested under thermal cycling and BB operating conditions (e.g. PbLi flow). Furthermore, preliminary scale-up to BB geometric dimension has been pursued. However, for the complete characterisation of the permeation barrier, the neutron damage should be taken into account and the impact of neutron irradiation on the PRF needs to be confirmed. Indeed, a damage dose rate up to 10 dpa/fpy should be reached and performances in terms of permeation reduction, corrosion mitigation and structural integrity of the coating should be demonstrated. Applicability to industrial-scale on complexes geometries and big dimension components as well as compatibility with manufacturing process (including, e.g. EUROFER heat treatment, welding, etc.) should furthermore be assessed in the Concept Phase.

Concerning the CPS system, several technological solutions, already existing in other power plants, have been identified. They can be used both for Water and Helium-cooled DEMO variants. In particular, regarding the water one, the results on T transport have demonstrated the necessity to have an in-line CPS. Two different solutions have been identified, one based on ITER design (column of 26 m height) with 20 kg/h of by-pass mass flow rate and one based on DTRF (the building is expected to be 35 m long, 25 m wide, 38 m height) operating in CANDU reactors in Ontario with a by-pass mass flow rate of 360 kg/h. Concerning the HCPB DEMO variant, two different processes are proposed for the removal of hydrogen isotopes: one is based on the scale-up of the "conventional" process used in fission and also in ITER CPS, and another relies on the use of novel NEG materials. The operating parameters identified for these options are CPS by-pass mass flow rate between 2 and 4 kg/s with an efficiency between 80 and 95%. Further efforts will be dedicated, during the Concept Design Phase, to the identification of the optimal working points.

Several sensitivity studies on T permeation from the plasma side [42, 43] have been performed. Although the uncertainties are still high, it has been demonstrated that the T retention (in the order of hundreds of grams) can have a big impact on the performances of the fuel cycle. Therefore, further analyses should be performed to investigate the possibility of reducing the Tungsten thickness minimising the T needed to saturate the structures during the start-up or that can be mobilizable during an accident. Hence, it should be addressed with high priority during the Concept Design Phase.

Concerning the sensitivity analyses on *T* permeation related to the Water-cooled DEMO variant, it has demonstrated the necessity to use an in-line CPS with a by-pass mass flow rate up to 360 kg/h for minimising the T concentration in the coolant and, therefore, to reduce the contamination of the secondary system. Moreover, limited effects have been found on the T management increasing both the TER extraction efficiency and the H_2 partial pressure in the coolant. On the contrary, the necessity of permeation barriers within the BB cooling structures with a PRF between 100 and 1000 has been confirmed. Furthermore, permeation barriers (PRF between 100 and 1000) are needed also on the PbLi loop piping together with guard pipes for reducing the T permeation into the tokamak building. Finally, the minimisation of the water leaks within the IHX/SG to reduce the T contamination of the secondary system should be further investigated.

T transport analyses on the Helium-cooled DEMO variant have demonstrated that the T permeation through the structures of the PHTS (i.e. piping) plays a more important role compared to the leakages in the tokamak building, as well as in the IHX. Indeed, the high T permeation through the PHTS piping introduces the necessity to install the permeation barriers. The same consideration in terms of excessive releases of T can be done for the HCPB TER system. Therefore, the use of permeation barriers with a PRF between 100 and 1000 and/or guard pipes in the TER loop to reduce the permeation into the tokamak building is envisaged. The studies have also indicated positive effects in reducing the T permeation when the performances of CPS and TER systems are increased in terms of mass flow rates and efficiencies. Finally, the use of steam into the purge gas and H_2 into the coolant has a positive effect on the overall T releases into the tokamak building, allowing for a reduction of the permeation rate by nearly five times.

In the Concept Design Phase, multi-parameter sensitivity analyses should be performed to investigate the joint effect of different parameters on the *T* transport and, therefore, on the determination of the T permeation rates and inventory. Moreover, an intense experimental campaign is planned in order to validate the tools used for the analyses.

Regarding the fuel cycle, the total throughput requiring treatment in the tritium plant together with several parameters related to the fuel cycle itself affect the *T* inventory to be managed. This is directly linked, of course, to the BB variants and the accompanying ancillary systems and has a direct effect on the TBR performances (1.03 – 1.05) that need to be achieved by DEMO. Furthermore, the TBR is also impacted by the

auxiliary systems installed within the VV. Indeed, the studies have shown that the TBR decrease due to the allocation of all IVCs is about 11%. Therefore, depending on the required TBR_{req} value adopted in the DEMO project (assumed range being 1.03–1.05) the target TBR can vary between 1.13 and 1.17 accounting for the impact of the integration of the auxiliary systems.

Concerning the VVPSS, during the Pre-Concept Design Phase, the ITER experience has been considered from the beginning. Indeed, for the preliminary design of the VVPSS, it has been assumed to have different tanks and to position them at the lower building level. This has been done to minimise, in case of a seismic event, the seismic forces and the sloshing response of the expansion tanks. Furthermore, several studies have been performed to assess the main VVPSS design driving factors. They are:

- Limiters protection function. This assumption has a big impact on the VVPSS design affecting both the sizing and the number of the RDs as well as the volume of the ETs. The demonstration of this limiter function will allow neglecting the worst-case scenario releasing the constraints to be considered for the VVPSS design.
- Plasma disruption event in case of rupture of feeding pipe in the upper port. The behaviour of the plasma should be further investigated to assess both the affected FW surface and the loads exerted on it.
- Dynamic behaviour during In-Vessel LOCA. The studies demonstrate that the pressure can locally reach values around 0.2 MPa jeopardising systems like the diamond windows. Therefore, further investigations should be performed on the propagation of the pressure wave to check the pressure evolution locally with 3D models, as in particularly unlucky scenarios (e.g. rupture in front of the diamond window) the suppression system designed for the "average" value using system codes may not be effective.
- Increment of the heat transfer to reduce the dimension of the expansion volume. The use of distribution header and spargers for the WCLL VVPSS variant or the use of an in-pool heat exchanger for the HCPB VVPSS allow reducing the overall volume needed to expand the fluid having a positive effect also on the peak pressure within the VV. However, further studies should be performed considering other scenarios and to detail the design.
- Use of IVs. In the WCLL PHTS, although the results show a positive effect on VV peak pressure and water inventory reduction, the use of IVs on the PHTS should be carefully evaluated. Indeed, having an active role during the accident in the minimization of the peak pressure and water inventory, they perform an important safety function. This means that they have to be redundant (i.e. high number of valves) increasing the complexity of the integration in the PHTS. Finally, in particular, for the IVs installed on hot/cold legs, the size of the pipe where the IVs should be installed poses manufacturability issues. The same effect, in terms of reduction of the released water inventory, can be obtained by increasing the number of WCLL PHTS loops. Concerning the Helium-cooled DEMO variant, the use of IVs is not useful to mitigate the release of inventory within the VV.
- The discharged area within the VV. For both VVPSS variants, a big opening in the VV should be foreseen in particular when the worst-case scenario is considered. In the case of the WCLL VVPSS, the sensitivity analyses show that an overall discharged surface of 8.6 m^2 is required to keep the pressure peak just below the limit of 2 bar. This is mainly due to the huge water inventory that is released within the VV (i.e. the sum of the FW and BZ loop inventories). Therefore, further activities should be dedicated to studying the increment of the number of FW and BZ loop taking into account the BoP performances as well as the VVPSS ones.
- H_2 formation and dust transported within the VVPSS. Preliminary studies have been performed to address the source term (e.g. hydrogen isotopes, ACPs, and tungsten dust) transported within the VVPSS. Additional studies have been performed in [52] and [53]. However, these results have not been used to determine the design of the H/T Passive Recombiner as well as for the determination of the requirements for the VVPSS. Therefore, in future activities, efforts should be dedicated to this topic and design activities on the H/T Passive Recombiner should be performed.

CRediT authorship contribution statement

G.A. Spagnuolo: Conceptualization, Methodology, Writing – original draft, Writing – review & editing, Supervision. **R. Arredondo:** Methodology, Investigation. **L.V. Boccaccini:** Supervision, Project administration. **P. Chiovaro:** Methodology, Investigation. **S. Ciattaglia:** Supervision. **F. Cismondi:** Conceptualization, Supervision. **M. Coleman:** Methodology, Investigation. **I. Cristescu:** Methodology, Investigation. **S. D'Amico:** Methodology, Investigation. **C. Day:** Methodology, Investigation. **A. Del Nevo:** Methodology, Investigation. **P.A. Di Maio:** Methodology, Investigation. **M. D'Onorio:** Methodology, Investigation. **G. Federici:** Supervision, Project administration. **F. Franza:** Methodology, Investigation. **A. Froio:** Methodology, Investigation. **C. Gliss:** Methodology, Investigation. **F.A. Hernández:** Methodology, Investigation. **A. Li Puma:** Supervision. **C. Moreno:** Methodology, Investigation. **I. Moscato:** Methodology, Investigation. **P. Pereslavtsev:** Methodology, Investigation. **M.T. Porfiri:** Supervision. **D. Rapisarda:** Supervision. **M. Rieth:** Supervision. **A. Santucci:** Methodology, Investigation. **J.C. Schwenzer:** Methodology, Investigation. **R. Stieglitz:** Supervision. **S. Tosti:** Supervision. **F.R. Urgorri:** Methodology, Investigation. **M. Utili:** Methodology, Investigation. **E. Vallone:** Methodology, Investigation.

Declaration of Competing Interest

The authors declare that they have no known competing financial interests or personal relationships that could have appeared to influence the work reported in this paper.

Acknowledgments

This work has been carried out within the framework of the EUROfusion Consortium and has received funding from the Euratom research and training programm 2014–2018 and 2019–2020 under Grant agreement No 633053. The views and opinions expressed herein do not necessarily reflect those of the European Commission.

References

[1] G. Federici, et al., The EU DEMO staged design approach in the pre-concept design phase, Fus. Eng. Des. (2021) no. This issue.
[2] G. Federici, et al., Overview of the DEMO staged design approach in Europe, Nucl. Fus. 59 (6) (2019), 066013.
[3] T. Donné, et al., European Research Roadmap to the Realisation of Fusion Energy, EUROfusion, 2018.
[4] A.J.H. Donné, The European roadmap towards fusion electricity, Philos. Trans. R. Soc. A Math. Phys. Eng. Sci. 377 (2141) (2019), 20170432.
[5] C. Bachmann, et al., Key design integration issues addressed in the EU DEMO pre-concept design phase, Fus. Eng. Des. 156 (2020), 111595.
[6] G.A. Spagnuolo, et al., Systems engineering approach in support to the breeding blanket design, Fus. Eng. Des. 146 (2019) 31–35.
[7] G. Bongiovì, et al., Systems engineering activities supporting the heating & current drive and fuelling lines systems integration in the European DEMO breeding blanket, Fus. Eng. Des. 147 (2019), 111265.
[8] L.V. Boccaccini, et al., Results and open challenges in the development of the EU DEMO breeding blanket, Fus. Eng. Des. (2021) this issue.
[9] A. Del Nevo, et al., Recent progress in developing a feasible and integrated conceptual design of the WCLL BB in EUROfusion project, Fus. Eng. Des. 146 (2019) 1805–1809.
[10] G.A. Spagnuolo, et al., Development of load specifications for the design of the breeding blanket system, Fus. Eng. Des. 157 (2020), 111657.
[11] L. Barucca, et al., Pre-conceptual design of EU DEMO balance of plant systems: objectives and challenges, Fus. Eng. Des. 169 (2021), 112504.

[12] I. Moscato et al., Tokamak coolant systems and power conversion system options, Pre-conceptual design of EU DEMO balance of plant systems: objectives and challenges, 2021 this issue.
[13] L. Barucca, et al., Status of maturation of critical technologies and systems design: balance of plant systems, Fus. Eng. Des. (2021) this issue.
[14] L. Barucca, et al., Status of EU DEMO heat transport and power conversion systems, Fus. Eng. Des. 136 (2018) 1557–1566.
[15] A. Santucci, et al., The issue of tritium in DEMO coolant and mitigation strategies, Fus. Eng. Des. 158 (2020), 111759.
[16] A. Santucci, et al., The coolant purification system in DEMO: interfaces and requirements, Fus. Eng. Des. 124 (2017) 744–747.
[17] F.A. Hernández, et al., Consolidated design of the HCPB breeding blanket for the pre-conceptual design phase of the EU DEMO and harmonization with the ITER HCPB TBM program, Fus. Eng. Des. 157 (2020), 111614.
[18] G.A. Spagnuolo, et al., A multi-physics integrated approach to breeding blanket modelling and design, Fus. Eng. Des. 143 (2019) 35–40.
[19] G.A. Spagnuolo, et al., Identification of blanket design points using an integrated multi-physics approach, Fus. Eng. Des. 124 (2017) 582–586.
[20] P. Chiovaro, et al., Investigation of the DEMO WCLL breeding blanket cooling water activation, Fus. Eng. Des. 157 (2020), 111697.
[21] P. Chiovaro, et al., Assessment of DEMO WCLL breeding blanket primary heat transfer system isolation valve absorbed doses due to activated water, Fus. Eng. Des. 160 (2020), 111999.
[22] P.A. Di Maio, et al., Private Communication: Final Report On Cooling Water Activation Assessment (EFDA_D_2MWLWF), EUROfusion, 2020.
[23] P.A. Di Maio, et al., Private Communication: Cooling Water Activation Assessment (EFDA_D_2N9GA3), EUROfusion, 2021.
[24] U. Fischer, et al., Neutronics requirements for a DEMO fusion power plant, Fus. Eng. Des. 98-99 (2015) 2134–2137.
[25] Pavel Pereslavtsev, et al., Analyses of the shielding options for HCPB DEMO blanket, Fus. Eng. Des. 156 (2020), 111605.
[26] M. Utili, et al., Development of anti-permeation and corrosion barrier coatings for the WCLL breeding blanket of the European DEMO, Fus. Eng. Des. 170 (2021), 112453.
[27] C. Alvani, et al., Effect of purge gas oxidizing potential on tritium release from Li-ceramics and on its permeation through 316L SS clads under irradiation (TRINE experiment), J. Nucl. Mater. 233-237 (1996) 1441–1445.
[28] A. Perujo, et al., Low pressure tritium interaction with Inconel 625 and AISI 316L stainless steel surfaces: an evaluation of the recombination and adsorption constants, Fus. Eng. Des. 31 (2) (1996) 101–108.
[29] D.P. Dautovich, The canadian fusion fuels technology project (CFFTP), Rev. Gen. Nucl. 1 (1) (1991) 87–90.
[30] H. Nakamura, et al., Case study on tritium inventory in the fusion DEMO plant at JAERI, Fus. Eng. Des. 81 (8) (2006) 1339–1345.
[31] H.A. Boniface, et al., Water detritiation system for ITER—evaluation of design parameters, Fu. Sci. Technol. 71 (3) (2017) 241–245.
[32] Y. Iwai, et al., Design study of feasible water detritiation systems for fusion reactor of ITER scale, J. Nucl. Sci. Technol. 33 (12) (1996) 981–992.
[33] A. Santucci et al., Private communication: TFV.OUTL-JUS-3-CD1 Development of a design solution for purification of helium coolant (EFDA_D_2MV73J), 2020.
[34] A. Ciampichetti, et al., The coolant purification system of the European test blanket modules: preliminary design, Fus. Eng. Des. 85 (10) (2010) 2033–2039.
[35] F. Franza et al., Private communication: collection of key parameters for DEMO breeding blankets tritium studies (EFDA_D_2L5SS4), 2017.
[36] E. Carella, et al., Private Communication: HCPB - Preliminary Tritium Transport Model Considering Simultaneous Permeation of Hydrogen/Deuterium and Tritium (EFDA_D_2NKAFU), EUROfusion, 2019.
[37] A. Santucci et al., Private communication: tFV-1.2-T5-D01_Helium/Water CPS draft pre-conceptual design (EFDA_D_2MAGF4), 2019.
[38] A. Busigin, et al., darlington tritium removal facility and station upgrading plant dynamic process simulation, Fus. Sci. Technol. 54 (2) (2008) 333–336.
[39] G.A. Esteban, et al., Diffusive transport parameters and surface rate constants of deuterium in Incoloy 800, J. Nucl. Mater. 300 (1) (2002) 1–6.
[40] F. Franza et al., Private communications: input specifications for tritium transport analyses at system level: DEMO 2017 baseline /HCPB blanket / PCS layout with IHTS + ESS (EFDA_D_2LHJHC) EUROfusion, 2020.
[41] P. Vladimirov, Private communication: BB.HCPB-JUS-2-CD1-R&D Beryllium-Beryllide development (EFDA_D_2P68VQ) EUROfusion, 2020.
[42] G.A. Spagnuolo, et al., Integration issues on tritium management of the European DEMO Breeding Blanket and ancillary systems, Fus. Eng. Des. 171 (2021), 112573.
[43] R. Arredondo, et al., Preliminary estimates of tritium permeation and retention in the first wall of DEMO due to ion bombardment, Nucl. Mater. Energy 28 (2021), 101039.
[44] M. Coleman, et al., DEMO tritium fuel cycle: performance, parameter explorations, and design space constraints, Fus. Eng. Des. 141 (2019) 79–90.
[45] J.C. Schwenzer, Operational tritium inventories in the EU-DEMO Fuel Cycle, to be submitted to Fus. Eng. Des.
[46] Pavel Pereslavtsev, et al., DEMO tritium breeding performances with different in-vessel components configurations, Fus. Eng. Des. 166 (2021), 112319.
[47] A. Zappatore, et al., 3D transient CFD simulation of an in-vessel loss-of-coolant accident in the EU DEMO fusion reactor, Nucl. Fus. 60 (2020), 126001.
[48] A. Froio, et al., Analysis of the effects of primary heat transfer system isolation valves in case of in-vessel loss-of-coolant accidents in the EU DEMO, Fus. Eng. Des. 159 (2020), 111926.
[49] M. D'Onorio, et al., Pressure suppression system influence on vacuum vessel thermal-hydraulics and on source term mobilization during a multiple first wall – blanket pipe break, Fus. Eng. Des. 164 (2021), 112224.
[50] S. D'Amico, Integral Approach to the Safety Design of the EU-DEMO Helium-Cooled Pebble Beds with Reference to the Associated Relevant Systems, Università degli Studi di Palermo, Palermo, 2020. Ph.D. thesis[Online]. Available, http://hdl.handle.net/10447/395442.
[51] E.U. Schlünder, et al., Heat Exchanger Design Handbook (no. v. 1; v. 2, pts. 1-2; v. 3, pts. 1-2; v. 4; v. 5, pts. 1-2), Hemisphere Publishing Corporation, 1983.
[52] M.T. Porfiri, Private communication: solutions to minimize in-vessel hydrogen and hydrogen/dust explosions: proposal and study (EFDA_D_2N458T), EUROfusion, 2018.
[53] M. D'Onorio, Private communication: hydrogen and dust explosion mitigation_ ENEA, IPP.CR (EFDA_D_2MRHG6), EUROfusion, 2019.